International Journal of
Extreme
Manufacturing

Aqueous electrolyte additives for zinc-ion batteries

Zhuoxi Wu, Zhaodong Huang, Rong Zhang, Yue Hou, Chunyi Zhi

View online: https://doi.org/10.1088/2631-7990/ad65ca

International Journal of Extreme Manufacturing

TOPICAL REVIEW • OPEN ACCESS

Aqueous electrolyte additives for zinc-ion batteries

To cite this article: Zhuoxi Wu *et al* 2024 *Int. J. Extrem. Manuf.* **6** 062002

OPEN ACCESS
IOP Publishing | IMMT
International Journal of Extreme Manufacturing
Int. J. Extrem. Manuf. 6 (2024) 062002 (25pp)
https://doi.org/10.1088/2631-7990/ad65ca

Topical Review

Aqueous electrolyte additives for zinc-ion batteries

Zhuoxi Wu[1], **Zhaodong Huang**[1], **Rong Zhang**[1], **Yue Hou**[1] **and Chunyi Zhi**[1,2,3,4,*]

[1] Department of Materials Science and Engineering, City University of Hong Kong, Kowloon 999077, Hong Kong Special Administrative Region of China, People's Republic of China
[2] Hong Kong Institute for Advanced Study, City University of Hong Kong, Kowloon 999077, Hong Kong Special Administrative Region of China, People's Republic of China
[3] Hong Kong Institute for Clean Energy, City University of Hong Kong, Kowloon 999077, Hong Kong Special Administrative Region of China, People's Republic of China
[4] Centre for Advanced Nuclear Safety and Sustainable Development, City University of Hong Kong, Kowloon 999077, Hong Kong Special Administrative Region of China, People's Republic of China

E-mail: cy.zhi@cityu.edu.hk

Received 12 October 2022, revised 19 August 2023
Accepted for publication 18 July 2024
Published 1 August 2024

Abstract

Because of their high safety, low cost, and high volumetric specific capacity, zinc-ion batteries (ZIBs) are considered promising next-generation energy storage devices, especially given their high potential for large-scale energy storage. Despite these advantages, many problems remain for ZIBs—such as Zn dendrite growth, hydrogen evolution, and Zn anode corrosion—which significantly reduce the coulomb efficiency and reversibility of the battery and limit its cycle lifespan, resulting in much uncertainty in terms of its practical applications. Numerous electrolyte additives have been proposed in recent years to solve the aforementioned problems. This review focuses on electrolyte additives and discusses the different substances employed as additives to overcome the problems by altering the Zn^{2+} solvation structure, creating a protective layer at the anode–electrolyte interface, and modulating the Zn^{2+} distribution to be even and Zn deposition to be uniform. On the basis of the review, the possible research strategies, future directions of electrolyte additive development, and the existing problems to be solved are also described.

Keywords: zinc-ion battery, electrolyte additives, solvation structure, solid electrolyte interphase protection layer, Zn dendrites, H_2 evolution

---

[*] Author to whom any correspondence should be addressed.

2631-7990/24/062002+25$33.00

1. Introduction

Fossil fuels play a dominant role in daily life activities and production processes over the past few decades. Because the supplies of these fuels are decreasing and the resulting pollution is becoming increasingly severe, scholars worldwide are focused on searching for alternative clean energy [1, 2]. Electrochemical energy storage devices, such as rechargeable batteries and supercapacitors, play a critical role in storing clean energy, which is mostly intermittent in nature. Researchers have developed numerous types of rechargeable lithium-ion battery (LIB) and have realized their practical applications [3–5]. However, limited lithium resources, safety problems, and high cost have hampered the application of LIBs as large-scale energy storage devices [2, 6, 7]. Potassium and sodium have similar chemical properties to lithium and are abundant in the earth, but potassium-ion batteries and sodium-ion batteries exhibit safety issues due to their flammable electrolytes [8]. Aqueous zinc-ion batteries (AZIBs) are considered one of the most promising advanced energy storage technologies because of the large reserves of zinc and the batteries' high theoretical capacity, high volumetric specific capacity, and low redox potential [9–12]. In addition to these advantages, AZIBs are completely safe and have high ion conductivity resulting from their aqueous electrolyte [13, 14].

The zinc-ion batteries (ZIBs) currently being investigated are rechargeable batteries and can thus be categorized as 'secondary batteries' [15, 16]. They comprise a cathode, an anode, electrolyte, separators, and other components [17–19]. The cathode is made from host materials that can store Zn^{2+}, including vanadium-based compounds, manganese-based compounds, and Prussian blue analogs [20, 21]. The anode is made from zinc that is reversibly stripped from and deposited on the anode [22, 23]. The electrolyte is a solution containing Zn^{2+}, including an alkaline solution or a neutral or mildly acidic solution (usually $ZnSO_4$ solution) [24]. Depending on the electrolyte used, the energy storage mechanism of ZIBs includes the Zn^{2+} intercalation mechanism, the H^+ and Zn^{2+} dual-ion intercalation mechanism, the reversible chemical reaction mechanism of charge transfer, or the coordination reaction mechanism of Zn and a positive organic material [25, 26].

When a ZIB is discharged, the Zn anode loses electrons, resulting in the formation of Zn^{2+} ions, which rapidly diffuse into the electrolyte and become embedded in the cathode. During the charging process, the opposite process occurs; Zn^{2+} ions are released from the cathode into the electrolyte, and after diffusing to the anode surface, they gain electrons and are deposited on the anode. Similar to LIBs, ZIBs are a type of 'rocking chair' battery.

When a Zn anode is used with an aqueous electrolyte, many adverse effects occur [13]. The electrolytes used in aqueous ZIBs usually have a neutral pH or are slightly acidic, and zinc metal is thermodynamically unstable when in contact with such electrolytes [27]. Therefore, many side reactions inevitably occur at the Zn anode during the electrochemical battery process, resulting in electrode corrosion, hydrogen evolution, Zn dendrite formation, and the formation of useless by-products, which have detrimental effects on the battery and may result in battery failure [28–30] (figure 1(a)).

The water molecules present in a traditional aqueous electrolyte can be divided into two types: free and solvated [31–34]. In the most commonly used electrolyte, which is 2 $mol\cdot l^{-1}$ $ZnSO_4$, the ratio of Zn^{2+} to water is 1:56, which means that water molecules surround each Zn^{2+} ion in the electrolyte. According to calculations, each Zn^{2+} ion couples with six free water molecules, forming a solvation sheath structure, and this structure exists as close ion pairs denoted as $[Zn(H_2O)_6]^{2+}$ [35, 36]. Charge carriers diffuse at the electrolyte-anode interface in this form, and the desired reaction at this interface is accompanied by a side reaction and the hydrogen evolution reaction (HER). During the stripping-plating process, water molecules in the solvation sheath tend to dissociate into H^+ and OH^-. The dissociated H^+ accumulates on the anode surface and induces hydrogen evolution. Generally, the HER is a two-step reaction in traditional weakly acidic electrolytes. First, a proton accumulates on the anode surface after it receives one electron; this is called the Volmer reaction [37]:

$$A + H^+ + e^- \rightarrow AH_{ads}. \qquad (1)$$

Subsequently, depending on the concentration of intermediate hydrogen atoms H^+, the reaction involving the desorption of H_2 molecules progresses through one of two parallel routes: the Heyrovsky reaction (equation (2)) or Tafel reaction (equation (3)),

$$AH_{ads} + H^+ + e^- \rightarrow A + H_2\uparrow \qquad (2)$$

$$2AH_{ads} \rightarrow 2A + H_2\uparrow. \qquad (3)$$

More importantly, once H^+ has been consumed, the remaining OH^- ions accumulate on the anode surface, which increases the local pH (figure 1(b)), exacerbating the formation of by-products $[Zn_4SO_4(OH)_6\cdot xH_2O]$; these by-products hinder ion and electron diffusion and reduce the reversibility of the Zn anode. Moreover, these useless by-products are unevenly distributed on the anode, further facilitating the growth of Zn dendrites [6, 38–40].

In most situations, Zn dendrites are caused by uneven Zn deposition during stripping-plating. Because the electrolyte microenvironment surrounding the anode is complex, Zn dendrite growth is unavoidable. The uneven distribution of the electric field and the irregular deposition of zinc ions further lead to the 'tip effect' [41–44]. Once protuberances have begun to form, they grow uncontrollably and finally become dendrites, which reduce the cycling stability of ZIBs and cause short circuits [45, 46].

In addition to the electric field distribution, many factors including the distribution of Zn^{2+} in the electrolyte and the flatness of the Zn anode influence the microenvironment at the anode–electrolyte interface. The solid electrolyte interphase (SEI) plays a crucial role during the Zn stripping-plating process [47]. A unique SEI on the surface of the Zn anode influences Zn deposition behavior in many ways. For example, Zn^{2+} tends to be distributed more evenly on anodes with an

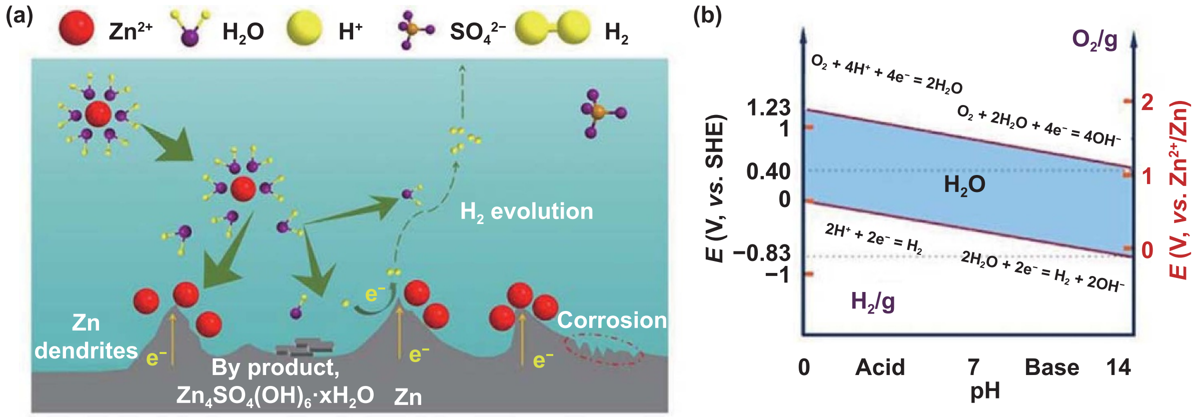

Figure 1. Schematic of zinc anode site reactions and the pourbaix diagram for Zn^{2+}. (a) Schematic diagram of Zn^{2+} solvation structure and de-solvation process, and the corresponding issues caused by the free water derived from solvation shell. (b) Pourbaix diagram for 10^{-6} $mol\cdot l^{-1}$ Zn^{2+}.

SEI [48]. Additionally, in the presence of an SEI, transfer kinetics at the electrolyte-anode interface are suppressed, which prevents the uneven distribution of Zn^{2+} on the anode surface and the growth of Zn dendrites.

Therefore, regulating the solvation structure of Zn^{2+} in the electrolyte and introducing a (quasi-)SEI membrane can effectively improve the electrochemical performance of AZIBs in terms of inhibiting the HER and Zn dendrite growth and improving coulomb efficiency and cycling stability [35, 49]. Introducing an additive to the electrolyte has been demonstrated to optimize the Zn^{2+} solvation structure and induce the formation of a thick SEI layer. For instance, molecules with a higher Gutmann donor number (Donor number is a parameter used to measure one solvent's ability to solvate Lewis acids. Zero value of donor number is the negative enthalpy of solvent 1:1 coordinate with $SbCl_5$ in dilute solution in 1,2-dichloroethane) than water can replace the H_2O in the solvation structure [50–52]. Additives with appropriate highest occupied molecular orbital (HOMO) and lowest unoccupied molecular orbital levels can mediate the formation of an SEI membrane [53]. Aqueous electrolyte additives for ZIBs are receiving increasing research attention, and crucial research should be summarized, which would guide the further development of aqueous electrolyte additives. In the present review, the various aqueous electrolyte additives are comprehensively introduced, and the mechanisms through which they affect the solvation sheath structure are described.

2. Additives for optimizing the solvation sheath structure

The solvation sheath around Zn^{2+} ions and the presence of active water molecules on the anode surface contribute to the occurrence of the HER and other side reactions in ZIBs. Zn^{2+} desolvation and deposition occur only if the high energy barrier (289.3 $kcal\cdot mol^{-1}$) to disrupting the $[Zn(H_2O)_6]^{2+}$ structure is overcome [54–57]. Additives that can replace H_2O in the solvation sheath and suppress the activity of H_2O in the electrolyte and at the anode–electrolyte interface are excellent for inhibiting the HER and other side reactions [26, 58]. The development process of ZIB additives is shown in figure 2. Various electrolyte additives have been proposed for altering the solvation sheath structure, including organic, ionic liquid, and polymer additives (figure 3). Most of these additives are organic substances, which have more Gutmann donors than do water molecules and have low Zn^{2+} binding energy; they can combine with Zn^{2+} cations before water molecules do and replace water molecules in the electrolyte. The details of these types of additives are discussed in the following subsections.

2.1. *Dipole-molecule additive*

Organic additives are the most popular type of additive used to regulate the solvation structure around Zn^{2+} ions and to improve the performance of ZIBs. Organic additives form a unique solvation structure around Zn^{2+}, in which the solvation structure is bound more strongly to Zn^{2+} in the presence of electrolyte additives than in the absence of additives. Thus, by regulating the solvation structure, an organic additive can stabilize the dynamic thermal properties of Zn^{2+}, improving the electrochemical performance of the battery. However, different organic additives exert their effects through different mechanisms, and these mechanisms are influenced by many factors, such as molecular polarity, carbon chain length, and spatial configuration of the additive. Researchers tend to employ additives that have strong molecular polarity because the additive molecules can effectively compete with H_2O molecules.

Wang *et al* introduced dimethyl sulfoxide (DMSO) into dilute $ZnCl_2$ solution, wherein the DMSO coordinated with Zn^{2+} and displaced water molecules in the solvation sheath, because DMSO has a higher Gutmann donor number (29.8) than H_2O (18), as shown in figure 4(a). Because of the prior coordination of DMSO-Zn^{2+} and the strong DMSO–H_2O

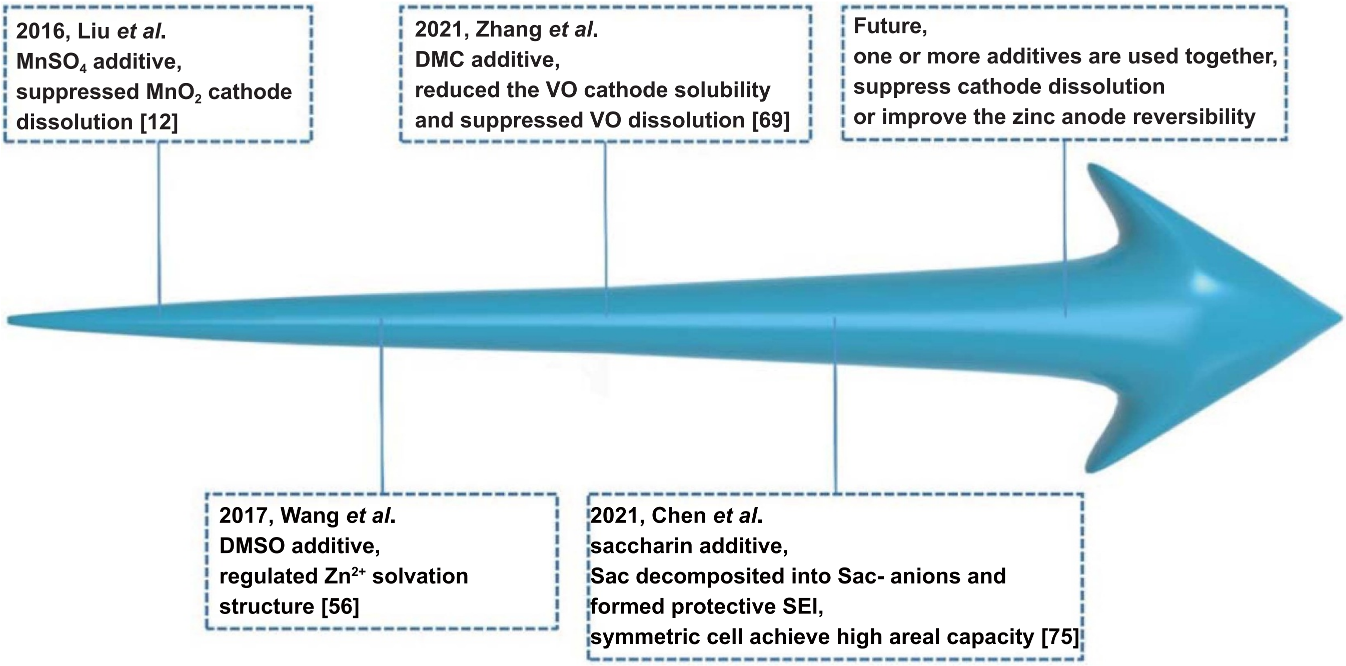

Figure 2. Roadmap of zinc ion battery electrolyte additives development progress.

bond, the decomposition of solvated H_2O was considerably inhibited. Furthermore, the deterioration of DMSO during the electrochemical process resulted in the formation of a novel SEI containing $Zn_{12}(SO_4)_3Cl_3(OH)_{15} \cdot 5H_2O$, $ZnSO_3$, and ZnS; this SEI prevented Zn dendrite growth and inhibited water decomposition [59]. These benefits led Zn||Zn symmetrical cells to exhibit higher extended cycling stability than those without the additive (figure 4(b)). Similar research on DMSO additives has been conducted by Wu *et al*. They found favorable dendrite growth inhibition and excellent subzero temperature performance when $ZnSO_4$ electrolyte contained a 20 volume ratio of DMSO (figure 4(c)). DMSO molecules have been proven to alleviate the parasitic reactions caused by H_2O in Zn^{2+} solvation structures. Moreover, due to the higher energy of DMSO absorption on the (002) lattice plane of Zn, the DMSO additive induces Zn^{2+} deposition more on the electrochemically stable (002) lattice plane than on other planes (figure 4(d)). The DMSO additive also reduces freezing point of an aqueous electrolyte. Consequently, researchers have reported that Zn/MnO_2 batteries can be cycled stably for more than 3000 times at 20 °C and 300 times at −20 °C [66] (figures 4(e) and (f)). In brief, DMSO is a typical organic additive that has numerous Gutmann donors and can be used to regulate the Zn^{2+} solvation structure and boost the electrochemical performance.

Acetonitrile (AN) is also widely used as an additive in the electrolyte within AZIBs. Adding AN to the electrolyte results in major improvements in a battery's performance; it alters the Zn^{2+} solvation structure, prevents Zn dendrite growth, and considerably improves coulomb efficiency during stripping–plating. Hou *et al* added AN to 2M $ZnSO_4$ as an additive for ZIBs [60]. The AN additive enhanced the intermolecular adjunction between Zn^{2+} and H_2O/AN, leading to supersaturated atoms on the current collector. This further facilitated uniform Zn atom nucleation and smooth deposition on the Zn metal anode. By performing molecular dynamics (MD) simulation, Zhang *et al* also found that the addition of AN led to the transformation of the $[Zn(H_2O)_6]^{2+}$ solvent sheath in the traditional aqueous electrolyte into three other solvated structures $[Zn(H_2O)_5(AN)_1{}^{2+}$, $Zn(H_2O)_4(AN)_2{}^{2+}$, and $Zn(H_2O)_3(AN)_3{}^{2+}]$, which were stable throughout the simulation (figure 5(a)). Therefore, AN molecules could effectively attack the solvent sheath of Zn^{2+} and replace some of the water molecules surrounding these ions; this alteration of the solvation sheath structure led to compact and uniform Zn growth (figure 5(b)) and higher electrochemical performance, which corresponds with the experimental results. Shi *et al* developed a mixed electrolyte with AN as an additive (H_2O:AN ratio of 3:1), which achieved high coulomb efficiency [67]. They found that the addition of AN led to the shielding of free H_2O molecules and the formation of a stable phase layer at the anode–electrolyte interface (figure 5(c)), thus significantly suppressing hydrogen evolution and dendrite formation. Their Zn||Zn symmetric cells exhibited long-term cycling stability over 1300 h (figure 5(d)) and a low overpotential of 38 mV. In addition, other researchers have used AN as a solvent for ZIB electrolytes or as an additive for water-in-salt electrolytes [68, 69].

Alcohols have been proven to be effective as an additive; the most representative of these alcohols are methanol and ethylene glycol (EG), which are the most widely used in ZIB electrolytes. Alcohols tend to be miscible with water in any

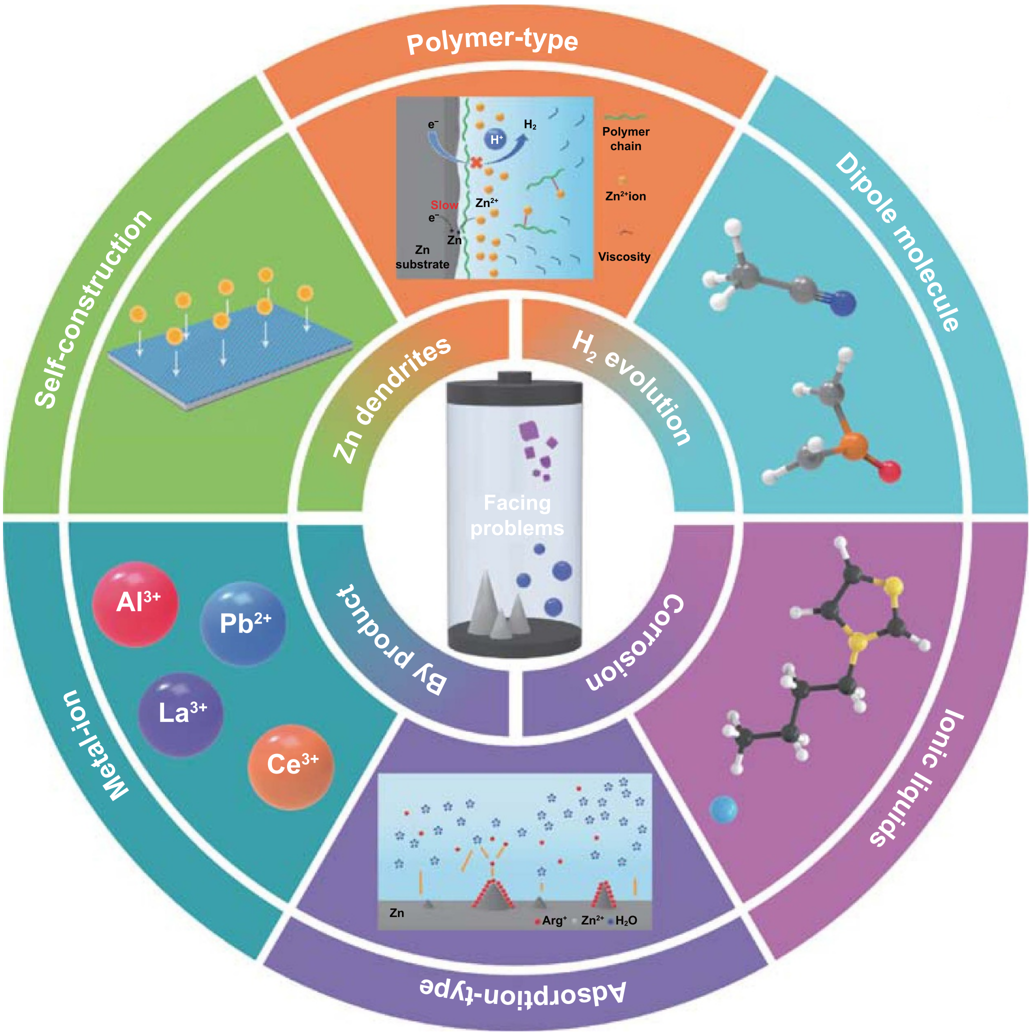

Figure 3. Overview of the facing issues and different types of electrolytes additives for zinc ion battery. Reprinted with permission from [59]. Copyright (2020) American Chemical Society. Reproduced from [60] with permission from the Royal Society of Chemistry. [61] John Wiley & Sons. ©2020 Wiley-VCH GmbH. Reprinted from [62], © 2021 Elsevier B.V. All rights reserved. [63] John Wiley & Sons. ©2021 Wiley-VCH GmbH. [64] John Wiley & Sons. ©2021 Wiley-VCH GmbH. [65] John Wiley & Sons. ©2020 Wiley-VCH GmbH. [35] John Wiley & Sons. ©2021 Wiley-VCH GmbH.

proportion, which makes them unique as additives. Hao *et al* reported on methanol as an electrolyte additive and discovered that it modified the Zn^{2+} solvation structure at the molecular level [70]. The Zn||Cu asymmetric cell assembled with electrolyte contained 50% methanol can operate under extreme conditions, and demonstrate excellent performance of 99.5% high CE at -10 °C and 98.1% high CE at 60 °C. Similar to the mechanism for DMSO, the added methanol molecules substituted solvated H_2O in the Zn^{2+} solvent sheath and free H_2O in the electrolyte (figure 6(a)) owing to their higher donor number (19) than that of H_2O (18); this led to the lower activity of H_2O and the weakened Zn^{2+} solvation effect, suppressing hydrogen evolution and side reactions. Qin *et al* added different volumes of EG to 3M $ZnSO_4$ electrolyte and discovered that the battery containing the electrolyte exhibited excellent electrochemical performance [71]. Through calculation, Pan *et al* found that as the EG content increased, the original solvation structure, composed of $[Zn(H_2O)_6]^{2+}$, changed into $[Zn(H_2O)_4(EG)]^{2+}$ and then into $[Zn(EG)_3]^{2+}$ (figure 6(b)). This evolution of the Zn^{2+} coordination environment led to decreased ionic diffusivity and increased nucleation overpotential, resulting in regular Zn deposition instead of the growth of massive dendrites (figures 6(c)–(e)). In addition, because fewer H_2O molecules were present in the solvation sheath, the activity of H_2O was weakened, and the side reactions were suppressed. A Zn||Zn symmetric coin battery containing 3M $ZnSO_4/H_2O$/68%vol EG achieved a long lifespan of 2668 h at 0.5 $mA\cdot cm^{-2}$, denoting outstanding electrochemical performance. The addition of EG was also discovered to reduce the electrolyte's freezing point (figure 6(d)), broadening the battery's working temperature range. Wang *et al* developed a localized and highly concentrated electrolyte, $ZnSO_4/H_2O$/EG, by introducing EG into $ZnSO_4$ electrolyte to serve as a 'water blocker'. They employed the electrolyte in Zn//phenanthrenequinone macrocyclic trimer batteries [61]. The addition of EG resulted in a unique solvation structure of Zn^{2+} ions, which suppressed the formation of hydrate by-products on the anode, restricted Zn^{2+} and SO_4^{2-} to create

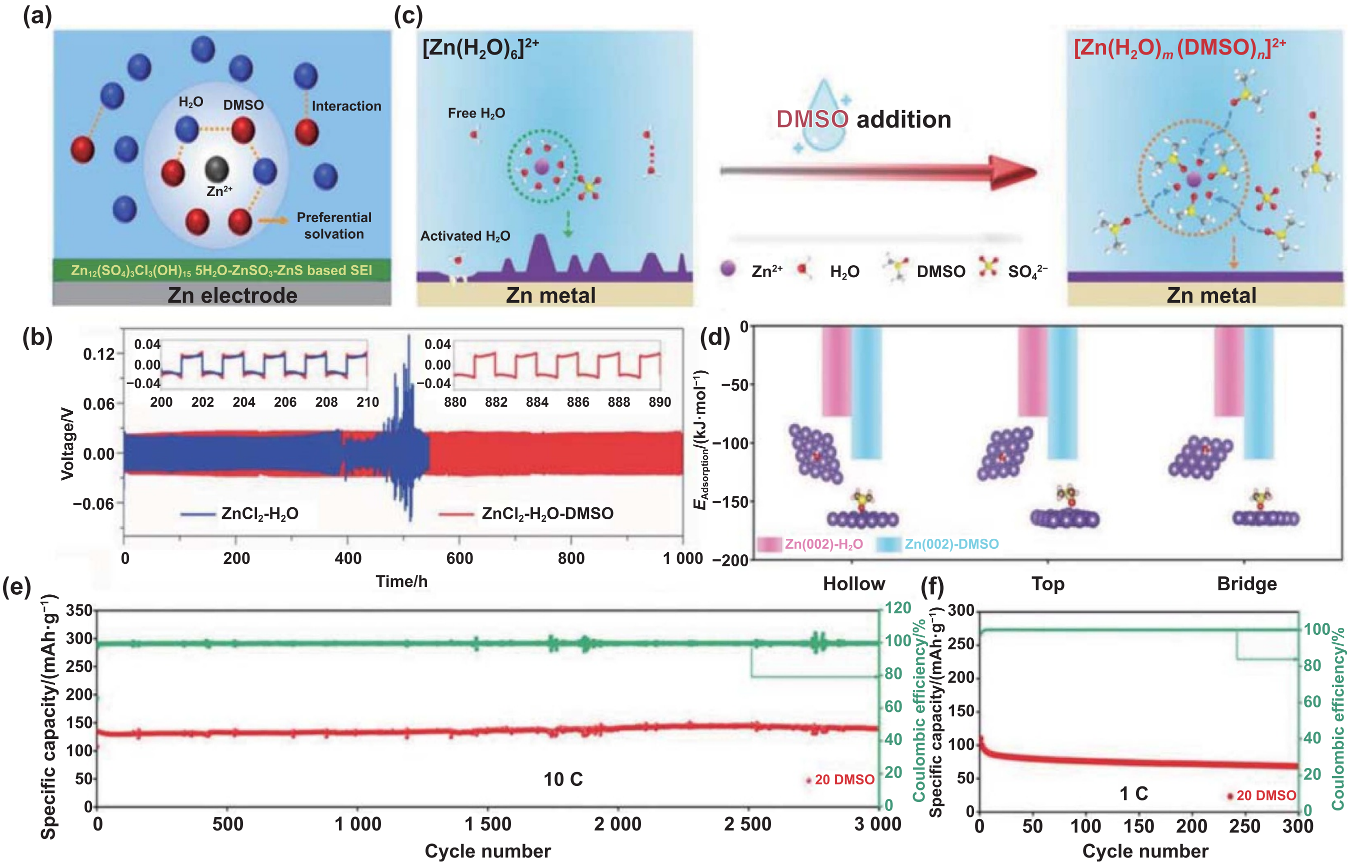

Figure 4. Figure of sulfone-based electrolyte additives. (a) Schematic of Zn^{2+} solvation structure and Zn anode surface passivation in DMSO containing electrolytes. Reprinted with permission from [59]. Copyright (2020) American Chemical Society. (b) Electrochemical performance of Zn||Zn symmetrical cells at 0.5 mA·cm^{-2} and 0.5 mAh·cm$^{-2.}$ Reprinted with permission from [59]. Copyright (2020) American Chemical Society. (c) Schematic illustration of changes of Zn^{2+} solvation structure from pure $ZnSO_4$ electrolyte to DMSO-containing electrolytes. [66] John Wiley & Sons. ©2021 Wiley-VCH GmbH. (d) Binding energy of Zn (002) plane with H_2O or DMSO. [66] John Wiley & Sons. ©2021 Wiley-VCH GmbH. (e) Cycle electrochemical performance Zn/MnO$_2$ full cell with 20 DMSO at 10 C. [66] John Wiley & Sons. ©2021 Wiley-VCH GmbH. (f) Cycle electrochemical performance of the Zn/MnO$_2$ full cell at −20 °C. [66] John Wiley & Sons. © 2021 Wiley-VCH GmbH.

a stronger ionic association ((figure 6(f)), and alleviated the undesirable HER, promoting dendrite-free Zn deposition and stripping. As a result, the Zn||PQ-MCT (phenanthrenequinone macrocyclic trimer) battery exhibited an excellent cycling stability (>8000 cycles).

Ether additives have also been applied to ZIB electrolytes. Feng *et al* introduced 1,4-dioxane (DX) to a pure $ZnSO_4$ electrolyte to modify the solvation structure of Zn^{2+} [72]. By performing density functional theory (DFT) calculations, they found that compared with water, the added DX molecules had higher Zn binding energy and greater affinity for Zn. DX tends to coordinate with Zn^{2+} and replaces some H_2O molecules in the solvation sheath, resulting in a more stable $Zn(H_2O)_n(DX)_m{}^{2+}$ solvation structure. Moreover, Liu *et al* found that DX molecules have greater affinity for the Zn (002) crystal plane than do water molecules (figure 7(a)). Therefore, the added DX molecules guided the orientation of Zn deposition along the (002) crystal plane, thus leading to nondendritic but dense lamellar deposits, which significantly improved the reversibility of the Zn anode (figure 7(b)). Finally, the Zn||Zn symmetric cell showed good cyclability of more than 600 h at 5 mA·cm^{-2}, 2.5 mAh·cm^{-2}. Cui *et al* employed a small amount of dimethyl ether (DME) as an additive in 2M $ZnSO_4$ [55]. The ether–oxygen bond in DME formed a hydrogen bond with water molecules (figure 7(c)), which significantly decreased the reactivity of free water. A stable Zn anode interface was formed, and the low reactivity of free water alleviated free-water-induced issues (HER, corrosion, etc). Nigatu *et al* also employed DME as an electrolyte additive and discovered that the wettability of the modified electrolyte was better than that of the original electrolyte [73]. With the addition of DME, a smooth and uniform deposition plane was observed after the first cycle (figure 7(d)). The same strategy was used by Du *et al* [62], who developed a $Zn(CF_3SO_3)_2$-based electrolyte with a 1,3-dioxolane (DOL) to water volume ratio of 1:1. The hybrid electrolyte featured a new H-bond network due to strong DOL-H_2O interaction. Because of the new constructed H-bond network (figure 7(e)), the modified electrolyte had a more negative hydrogen evolution overpotential but still had high conductivity of 30 mS·cm^{-1}, which significantly inhibited H_2 evolution on the anode and by-product formation. Therefore, the Zn||Zn symmetric cell with hybrid

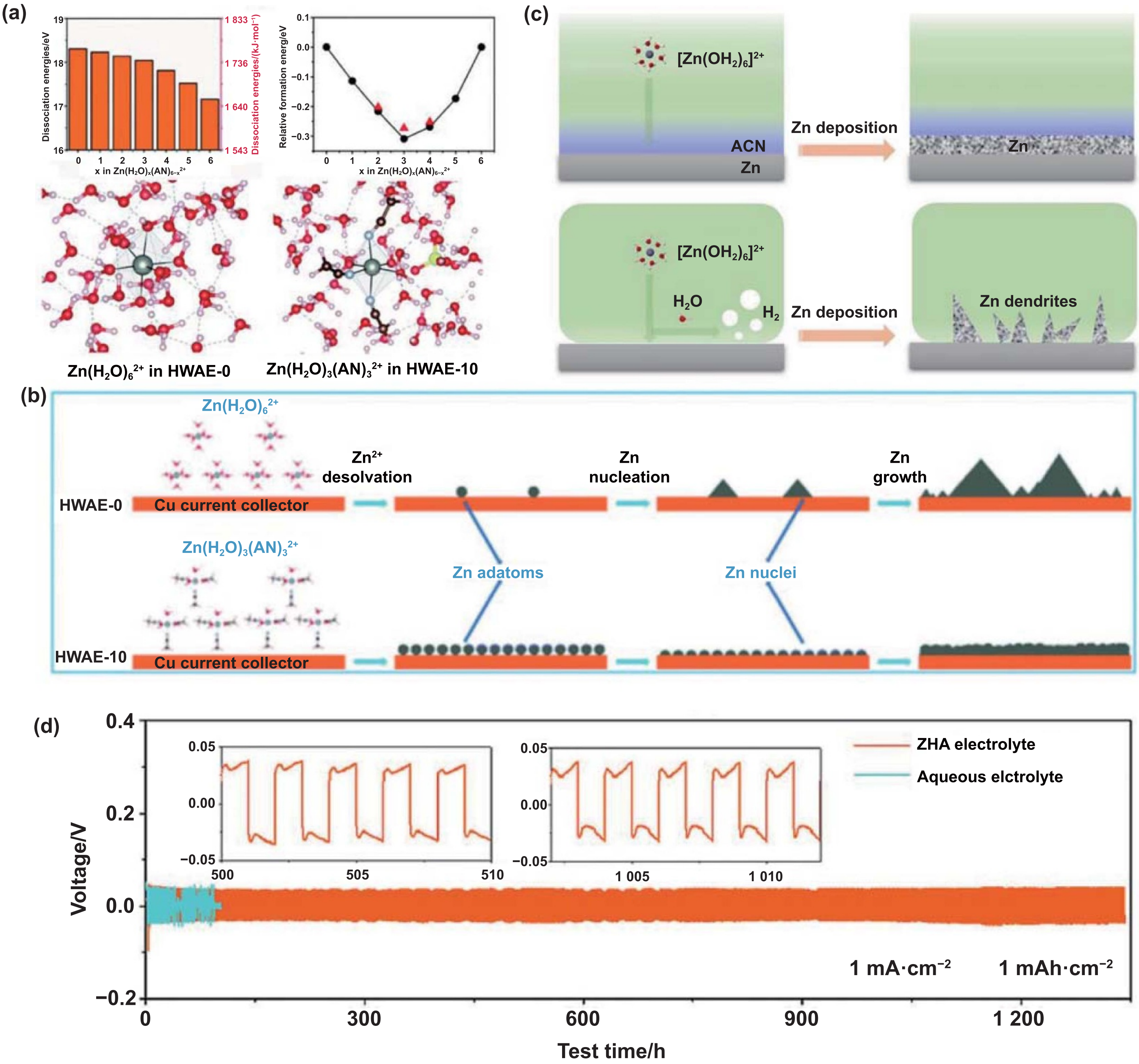

Figure 5. Figure of nitrile-based electrolyte additives. (a) Dissociation energies of the $Zn(H_2O)_x(AN)_{6-x}{}^{2+}$ complexes, pseudo phase diagram of $Zn(H_2O)_x(AN)_{6-x}{}^{2+}$ and snapshots of the AIMD simulations of HWAE-0 (no AN additive) and HWAE-10 (10% AN additive). Reproduced from [60] with permission from the Royal Society of Chemistry. (b) Conceptual diagram of Zn nucleation and growth process without AN additive and with AN additive. Reproduced from [60] with permission from the Royal Society of Chemistry. (c) Schematic illustration of Zn morphology evolution in AN-containing electrolyte and pure $ZnSO_4$ electrolyte. Reprinted from [67], © 2020 Elsevier Ltd. All rights reserved. (d) Long-term cycling performance of Zn/Zn symmetric cells with and without AN additive at 1 mA·cm^{-2} and 1 mAh·cm^{-2}. Reprinted from [67], © 2020 Elsevier Ltd. All rights reserved.

electrolyte could cycle stably for 1500 h at 0.5 mA·cm^{-2}, 0.5 mAh·cm^{-2}.

Researchers have also developed some other substances as additives in ZIB electrolytes. For example, Dong *et al* employed dimethyl carbonate (DMC) as an additive in 2M $Zn(CF_3SO_3)_2$ electrolyte to stabilize the electrochemistry of zinc ions in a ZIB [74]. MD simulation showed that when the ratio of water to DMC was 4:1, the first Zn^{2+} solvation sheath was occupied by 3.9 water molecules, 0.7 DMC solvent molecules, and 1.4 $CF_3SO_3{}^-$ anions, leading to a unique solvation structure: $Zn^{2+}[H_2O]_{3.9}[DMC]_{0.7}[CF_3SO_3]_{1.4}$ (figure 8(a)). The functional SEI greatly improved the performance of symmetric cells containing the modified electrolyte; the cells had a long lifespan of more than 600 cycles at 5 mA·cm^{-2}, 2.5 mAh·cm^{-2}, and they had a high average coulomb efficiency of 99.8% (figure 8(b)). The unique solvation structure facilitated the decomposition of coordinated Zn^{2+}-CF_3SO_3 and Zn^{2+}-DMC on the Zn anode surface, forming a ZnF_2–$ZnCO_3$-rich SEI layer (figure 8(c)) that inhibited parasitic reactions and dendrite growth.

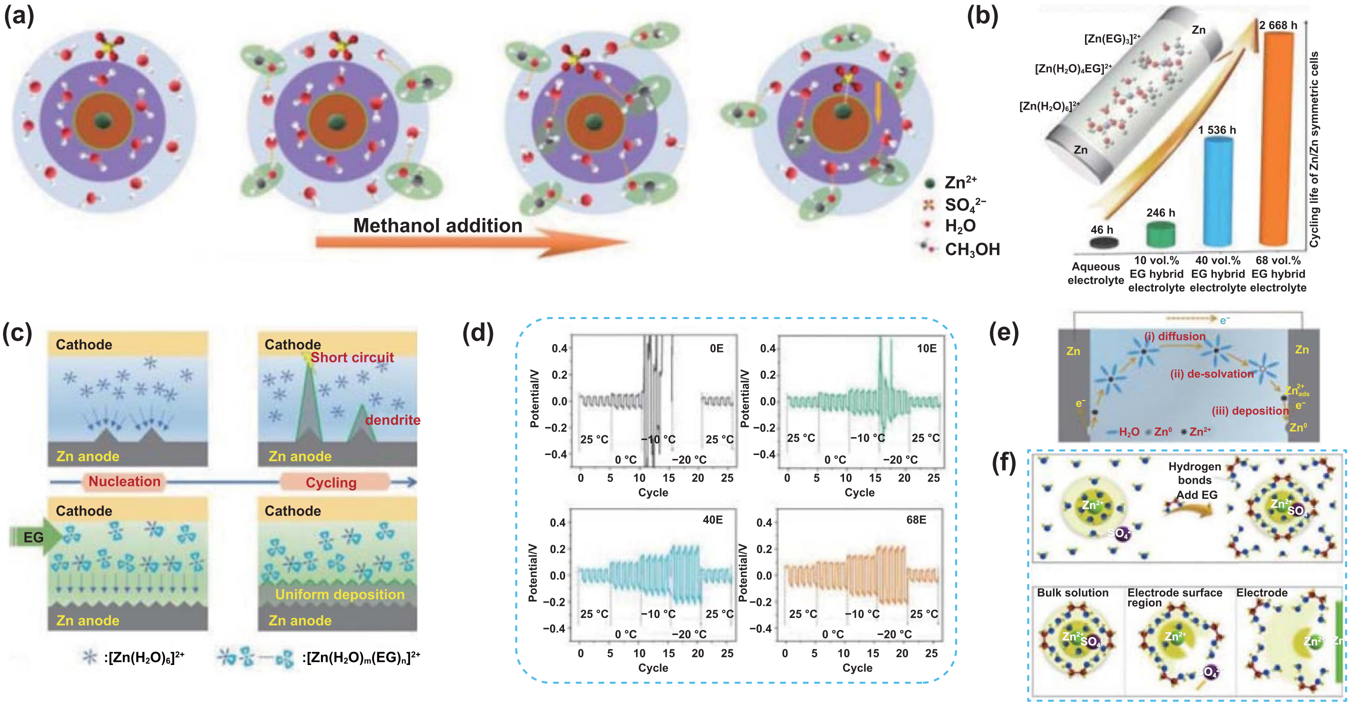

Figure 6. Figure of alcohol-based electrolyte additives. (a) Diagram of Zn^{2+} solvent structure evolution after adding methanol. [70] John Wiley & Sons. ©2021 Wiley-VCH GmbH. (b) Coordination number of EG in Zn^{2+} solvation structure for the electrolytes with different content of EG, and lifespan of Zn/Zn symmetric cells with EG containing electrolytes. Reprinted from [71], © 2020 Elsevier Ltd. All rights reserved. (c) Conceptual diagram of dendrite inhibition and deposition morphology in EG-containing electrolytes. Reprinted from [71], © 2020 Elsevier Ltd. All rights reserved. (d) Diagram of Zn deposition processes. Reprinted from [71], © 2020 Elsevier Ltd. All rights reserved. (e) Voltage figures for Zn/Zn symmetry cells at different temperatures. Reprinted from [71], © 2020 Elsevier Ltd. All rights reserved. (f) Solution structure and electrochemical mechanism of EG-based electrolyte. [61] John Wiley & Sons. ©2020 Wiley-VCH GmbH.

Luo *et al* used the chelating agent 2-bis(2-hydroxyethyl) amino-2-(hydroxymethyl)-1,3-propanediol (BIS-TRIS) to adjust the solvation structure of Zn^{2+}. The added BIS-TRIS also prevented Zn corrosion and side reactions on the anode. Scanning electron microscopy (SEM) images revealed that after Zn foil was soaked in the BIS-TRIS-containing electrolyte for 7 d, the foil was smoother; by contrast, after Zn foil was soaked in 2M $ZnSO_4$ electrolyte, a large amount of by-products were present on the Zn foil (figure 8(d)). The SEM image obtained after cycling revealed that when the BIS-TRIS additive was used, the morphology of deposited Zn was more even and smooth (figure 8(e)). Additionally, due to the chelated coordination of Zn^{2+}-BISTRIS, some Zn^{2+}-H_2O bonds in the Zn^{2+} solvent sheath were replaced by Zn^{2+}-BISTRIS [75]. The 2D diffusion of Zn^{2+} on the anode surface was restricted. The BIS-TRIS additive led to reductions of deposition kinetics and the transformation of deposition behavior, which suppressed the growth of dendrites (figure 8(f)). Because of the replacement of H_2O in the Zn^{2+} solvation sheath, the additive inhibited vigorous H_2 evolution. Therefore, a stable zinc metal anode interface was formed. The Zn‖Zn symmetric cell with BISTRIS additive demonstrated excellent long lifespan of 600 h at 5 mA·cm^{-2}, 5 mAh·cm^{-2}.

Wang *et al* employed tridentate citrate (Cit^{3-}) as an additive in an electrolyte and obtained good performance for ZIBs using the electrolyte [76]. The Cit^{3-} anion formed a unique chelate solvation structure, namely $[ZnCit(H_2O)_3]^-$, by chelating with Zn^{2+} (figure 8(g)). The addition of Cit^{3-} enabled the dehydration of the solvent sheath, passivating the remaining coordinated water and suppressing Zn^{2+} transfer kinetics; consequently, the distribution of Zn^{2+} was homogeneous, and the Zn anode remained free of dendrites.

Hou *et al* employed urea as an additive in the electrolyte [77]. As a potent ligand, urea formed a unique solvation structure, namely $[Zn(H_2O)_2(urea)_3]^{2+}$, in the electrolyte. Together with Zn^{2+}, the two coordinated H_2O molecules were cointercalated into the cathode material during discharge, which induced Zn^{2+} diffusion. Additionally, owing to the partial substitution of H_2O with urea, the solvated structure led to less damage to the structure of the cathode material and thereby prevented the disruption of this structure (figure 8(h)). The in-situ cathode-electrolyte interphase contributed by urea decomposition inhibited the dissolution of the cathode material, protecting the structure of the cathode material and improving the lifespan of the entire cell.

2.2. *Ionic-liquid-type additives*

Ionic liquids are also promising candidate additives in electrolytes in ZIBs. Zhang *et al* added 1-ethyl-3-methylimidazolium chloride to the traditional $ZnSO_4$ electrolyte [63] and found

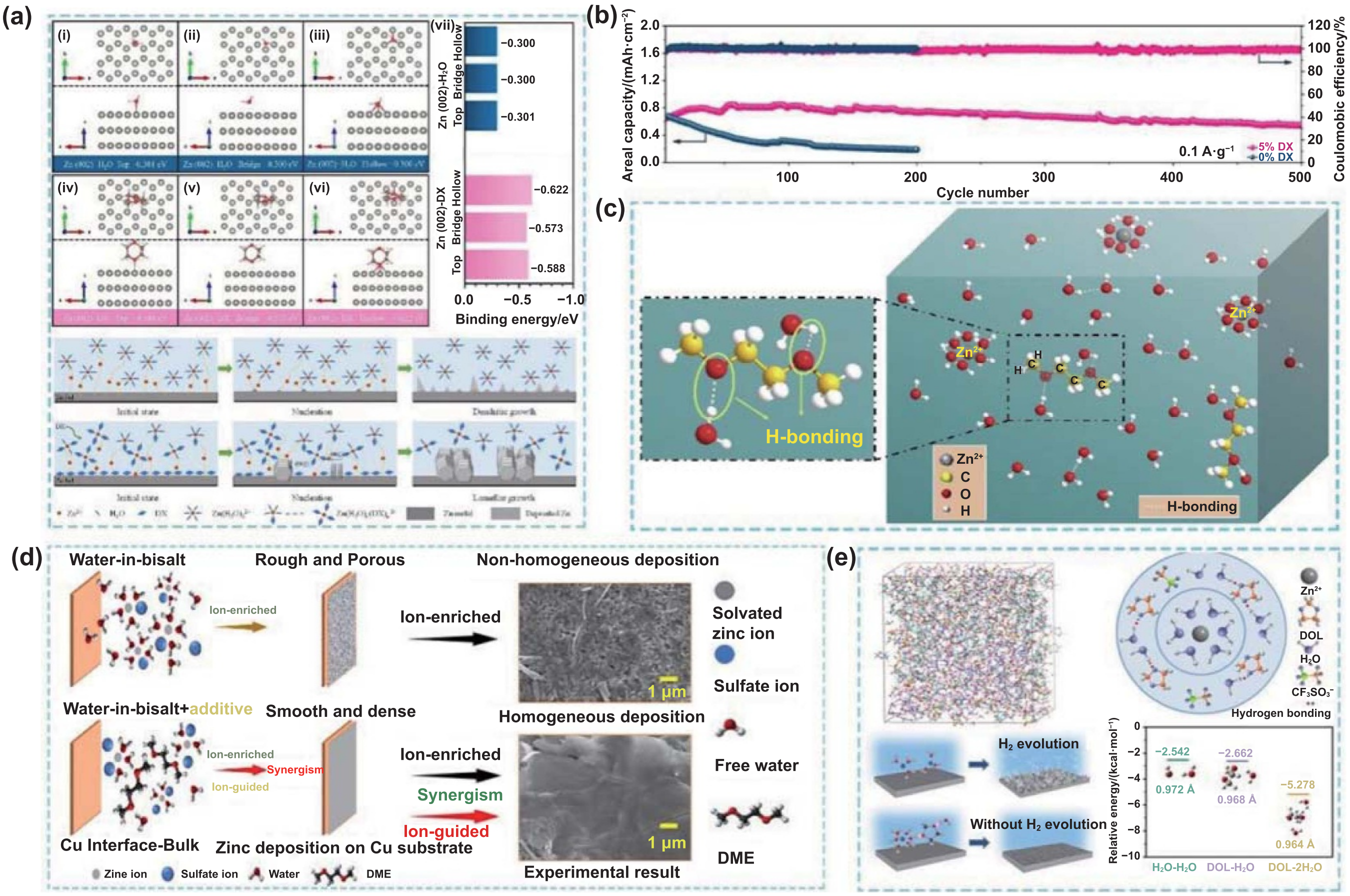

Figure 7. Figure of ether-based electrolyte additives. (a) Schematic diagram of the DX-guided deposition mechanism. Geometries of Zn (002) lattice plane with water molecules and DX molecules at top, bridge, and hollow sites; binding energy of Zn (002) lattice plane with H_2O and DX; and Zn deposition process in different electrolytes. Reprinted with permission from [72]. Copyright (2021) American Chemical Society. (b) Full cells electrochemical performance with and without DX additive, at current density of 0.1 $A\cdot g^{-1}$, showing high coulomb efficiency. Reprinted with permission from [72]. Copyright (2021) American Chemical Society. (c) Diagram of H-bonding in the aqueous electrolyte with low DME concentration. Reprinted from [55], © 2020 Elsevier Ltd. All rights reserved. (d) Scheme of functional 1,2-dimethoxy ethane additive in Zn||Cu half-cell and the corresponding SEM image. Reprinted from [73], © 2021 Elsevier B.V. All rights reserved. (e) Snapshot of the MD simulation cell for the DOL-containing electrolyte (50% DOL); Zn^{2+} solvation structure adapted from MD simulation; conceptual diagram of H_2 evolution prohibition by DOL additive; and relative binding energy for DOL with H_2O molecules obtained from DFT calculations. Reprinted from [62], © 2021 Elsevier B.V. All rights reserved.

that this additive transformed the original water-involved solvation structure of $Zn(H_2O)_6{}^{2+}$ into the anion-type anhydrous structure of $ZnCl_4^{2-}$ (figure 9(a)). Thanks to the strong binding between the anion and Zn^{2+}, HER was greatly suppressed, whereas the formation of dendrites was stopped, and the cell exhibited uniform zinc deposition and up to 99.9% coulomb efficiency (figure 9(b)). Wang *et al* added 1-methyl-1-ethylpyrrolidine bromide to a conventional electrolyte to obtain long-life ZIBs [78]. The presence of Br^- anions changed the primary Zn^{2+} solvation structure and reduced the overpotential of Zn^{2+} deposition. MEP^+ cations were adsorbed on protrusions on the zinc metal surface (figure 9(c)), forming an electrostatic shielding layer, inhibiting tip discharge, and guiding uniform deposition of Zn^{2+} ions. In addition to the above works, recently, Chen *et al* also reported an ionic liquid additive named 1-butyl-3-methylimidazolium trifluoromethanesulfonate ([BMIM]OTF) [79]. They added 0.5M [BMIM]OTF into 3M $Zn(CF_3SO_3)_2$ aqueous electrolyte and achieved a high-performance ZIB. With [BMIM]OTF additive, the Zn^{2+} solvation sheath is regulated. Besides, owing to the [BMIM]OTF molecules priorly absorbed on the Zn anode, an organic/inorganic hybrid SEI film was formed at the anode/electrolyte interface (figure 9(d)). Therefore, parasitic reaction on the anode surface and Zn corrosion are inhibited. The Zn||Zn symmetric battery shows good cyclability at 5 $mA\cdot cm^{-2}$, 25 $mAh\cdot cm^{-2}$, as shown in figure 9(e). Zhang *et al* also employed 1-butyl-3-methylimidazolium cation ($BMIm^+$ ion) as additive to improve the AZIBs performance (figure 9(f)) [80]. Different from Shi *et al*, they found that the added $BMIm^+$ cations would preferentially be absorbed on the (100) and (001) crystal plane of Zn, forcing the Zn^{2+} to deposit along the (002) crystal plane. The Zn deposited on the (002) crystal plane is evenly and ordered, and the Zn dendrites growth is significantly suppressed (figure 9(g)). As a result, the Zn||Zn symmetric cell exhibits a long lifespan of more than 1000 h at 10 $mA\cdot cm^{-2}$, 10 $mAh\cdot cm^{-2}$.

An ionic liquid additive dissociates into cations and anions in an aqueous electrolyte. These cations and anions interact

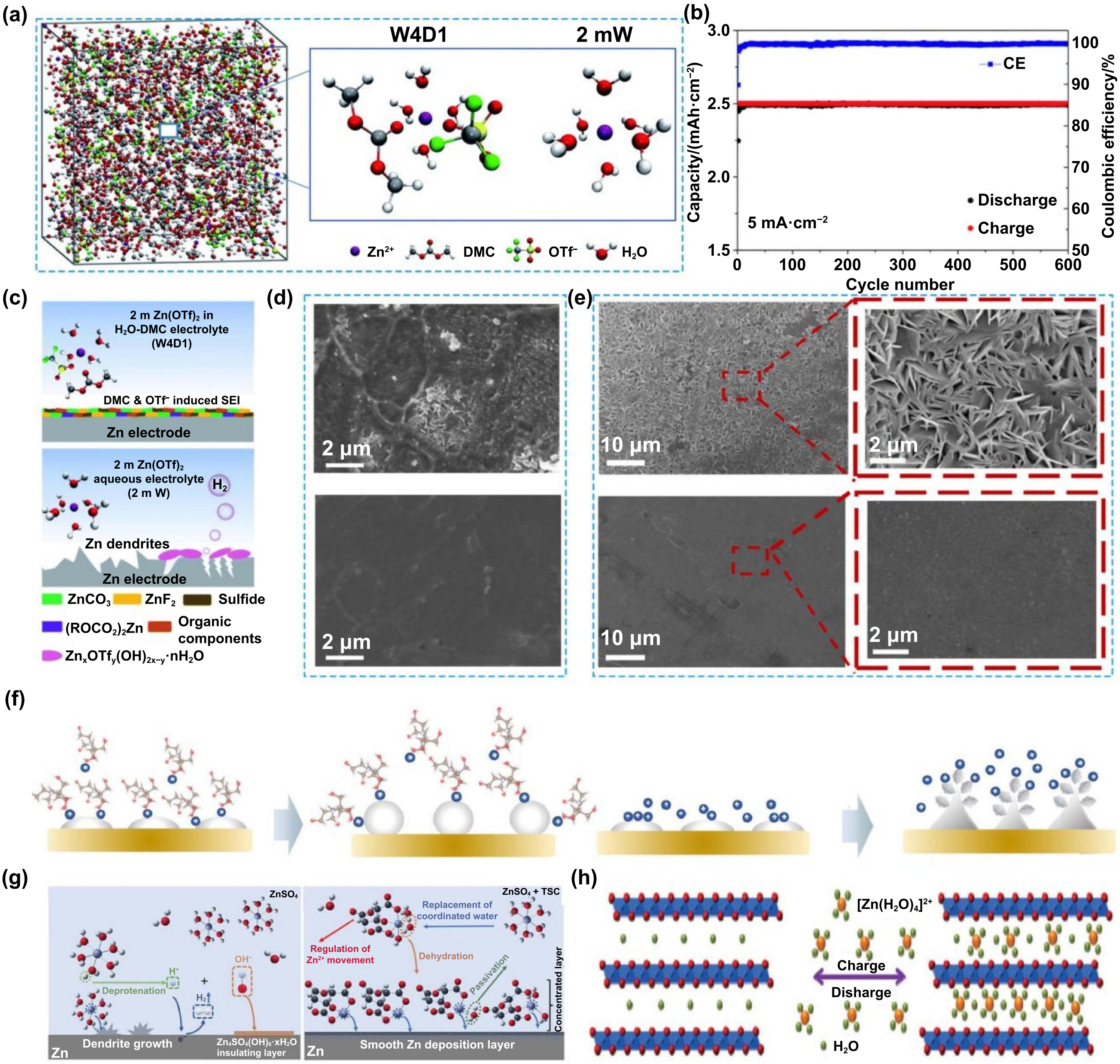

Figure 8. Figure of other dipole organic electrolyte additives. (a) Snapshot of the MD simulation cell for the DMC-containing electrolyte (W4D1, H_2O:DMC = 4:1), and the representative Zn^{2+}-solvation structures in W4D1 and pure $ZnSO_4$ aqueous electrolytes. Reproduced with permission from [74]. © 2021 The Author(s). Published by the Royal Society of Chemistry, CC BY-NC 3.0. (b) Cycling performance of the Zn/Ti half cell in DMC-containing electrolyte (W4D1 electrolyte) at 5 mA·cm^{-2} and the corresponding Coulombic efficiency. Reproduced with permission from [74]. © 2021 The Author(s). Published by the Royal Society of Chemistry, CC BY-NC 3.0. (c) Conceptual diagram of properties at Zn anode/electrolyte interface in W4D1 and 2 M $ZnSO_4$ electrolytes. Reproduced with permission from [74]. © 2021 The Author(s). Published by the Royal Society of Chemistry, CC BY-NC 3.0. (d) SEM image of Zn morphology after soaking in the electrolyte with and without BIS-TRIS additive for 7 d. Reprinted from [75], © 2021 Elsevier B.V. All rights reserved. (e) SEM image of Zn anode morphology after 10 cycles in the electrolyte with and without BIS-TRIS additive. Reprinted from [75], © 2021 Elsevier B.V. All rights reserved. (f) Schematic representation of spherical Zn deposition in electrolyte with BIS-TRIS additive and Zn dendrites growth in $ZnSO_4$ electrolyte. Reprinted from [75], © 2021 Elsevier B.V. All rights reserved. (g) Scheme of interfacial reactions on Zn surface in $ZnSO_4$ electrolyte without and with TSC additives. Reprinted from [76], © 2021 Elsevier B.V. All rights reserved. (h) Schematic of hydrated Zn intercalation process. [77] John Wiley & Sons. © 2020 WILEY-VCH Verlag GmbH & Co. KGaA, Wemheim.

with Zn^{2+} in the electrolyte in different ways, transforming the structure of the Zn^{2+} solvation sheath, inhibiting the activity of free water molecules, and preventing hydrogen evolution and Zn anode corrosion.

In conclusion, the additives that can alter the solvation structure are mainly organic molecules. Most of them exhibit solid polarity, meaning that they can attack the Zn^{2+} solvation sheath, replacing coordinated water molecules, reducing

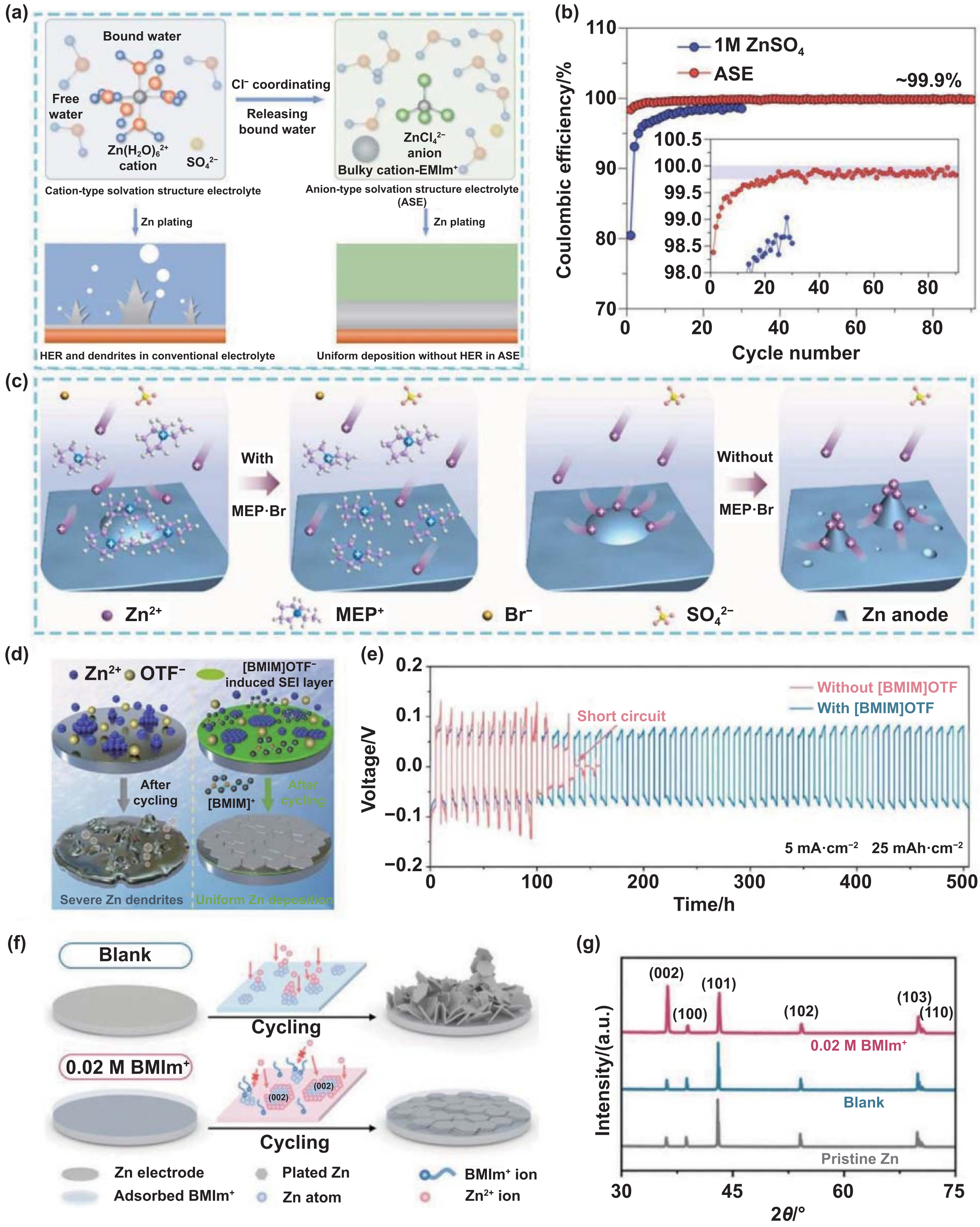

Figure 9. Figure of ionic liquid electrolyte additives. (a) Schematic of the new anion type $ZnCl_4^{2-}$ solvation structure, the bound water of Zn^{2+} is released by the coordination of Cl^-, and unique non-dendritic Zn plating pattern. [63] John Wiley & Sons. ©2021 Wiley-VCH GmbH. (b) Coulomb Efficiency of Zn||Cu batteries at 1 mA·cm^{-2}. [63] John Wiley & Sons. ©2021 Wiley-VCH GmbH. (c) Scheme of Zn deposition behavior in the electrolytes with and without MEP·Br. Reprinted from [78], © 2022 Elsevier Ltd. All rights reserved. (d) Schematic illustration of [BMIM]OTF additive stabilizing the Zn deposition process. Reprinted from [79], © 2022 Elsevier B.V. All rights reserved. (e) Cycling performance of Zn||Zn symmetric cell with [BMIM]OTF additive at 5 mA·cm^{-2} and 25 mAh·cm^{-2}. Reprinted from [79], © 2022 Elsevier B.V. All rights reserved. (f) Schematic of preferential growth of (002) plane induced by $BMIm^+$ ion during cycling of AZIBs. [80] John Wiley & Sons. ©2022 Wiley-VCH GmbH. (g) XRD patterns comparison of Zn anodes of pristine, after 30 cycles in blank electrolyte (short circuit) and 50 cycles in electrolyte with 0.02 m $BMIm^+$ additive. [80] John Wiley & Sons. © 2022 Wiley-VCH GmbH.

the activity of free H_2O, and inhibiting dendrite growth, HER, and corrosion. Organic additives are a promising choice in many cases, but they have several shortcomings. (1) The sizeable molecular radius of organic additives produces considerable steric hindrance, which reduces Zn^{2+} ion conductivity and suppresses Zn^{2+} transfer kinetics. (2) Although side reactions are inhibited when water molecules are substituted with organic additives, the strong coordination between additive molecules and Zn^{2+} leads to a higher energy barrier to Zn^{2+} desolvation, which makes Zn^{2+} desolvation less likely to occur, leading to higher nucleation overpotential and greater polarization. (3) As the content of an organic additive is increased, the water content of the electrolyte decreases, leading to safety hazard, the details are discussed in 4.3.

3. Additives promoting the formation of SEI/quasi-SEI film

Additives strongly affect the type of (quasi-)SEI membrane formed on the anode. This formation occurs through three types of mechanism: decomposition, adsorption, and metal ion mechanisms.

3.1. Self-construction of SEI additive

Huang *et al* proposed the addition of saccharin (Sac) to an electrolyte for adjusting the electrical double-layer interface on the negative electrode [81]. Experimental results indicated that Sac-dissociated anions rather than H_2O were adsorbed on the Zn metal surface, forming an H_2O-poor electrical double-layer interface (figures 10(a) and (b)). Moreover, owing to its low HOMO energy level, Sac tended to combine with electrons during cycling and dissociate into Sac^- anions. The decomposed Sac^- anions constructed a unique SEI on Zn anode, preventing H_2 evolution and some other side reactions and modulated Zn^{2+} deposition behavior. Consequently, the Zn||Zn symmetric cell with Sac additive showed outstanding performance with 2.75 Ah·cm^{-2} cumulative capacity at 10 mA·cm^{-2}, 10 mAh·cm^{-2}. Xi *et al* employed saccharin sodium as an ultra-low-concentration additive in 2M $ZnSO_4$ electrolyte (<1 g·l^{-1}) [82]. In their research, the dissociated saccharin anion assisted with Zn^{2+} transport in the electrolyte (figure 10(c)), guiding the uniform deposition of zinc during charging and discharging without any noticeable side reactions. The assembled zinc symmetric cell had a long lifespan of more than 3800 h at 5 mA·cm^{-2}, 8 mAh·cm^{-2} (figure 10(d)). DMSO, which has been described in the earlier text, was also discovered to lead to the formation of creating a unique SEI protection film on the anode surface. Cao *et al* revealed that the added DMSO, which had a low HOMO energy level, reacted with electrons and then decomposed, forming a novel SEI containing $Zn_{12}(SO_4)_3Cl_3(OH)_{15} \cdot 5H_2O$, $ZnSO_3$, and ZnS. The SEI not only prevented side reactions but also suppressed Zn dendrite growth [59].

Inspired by the bioadhesion principle, Zeng *et al* generated a stable polydopamine interfacial layer on a Zn anode by adding dopamine to the electrolyte [83] (figure 10(e)). The dopamine-induced SEI exhibited numerous features owing to its abundant functional groups and excellent hydrophilicity. The SEI not only regulated Zn nucleation on the anode but also improved ionic conductivity and prevented interfacial side reactions. The battery fabricated by Guo *et al* demonstrated outstanding stability at 30 mA·cm^{-2}, 30 mAh·cm^{-2} (figure 10(f)).

The aforementioned additives form an SEI at the anode–electrolyte interface through chemical decomposition or chemical self-construction. They form an SEI through two main mechanisms: in the first mechanism, the additives combine with electrons due to their low HOMO energy level, and in the second mechanism, they self-decompose or self-polymerize. Regardless of the route, the formed SEI has considerable potential to protect the Zn anode from parasitic reactions and prevent uneven Zn dendrite growth. Introducing additives that can form a novel SEI on the Zn anode surface is a convenient and effective way of protecting the Zn anode, but in many cases, researchers have not considered the Zn deposition overpotential when adding additives. Excessive overpotential is unfavorable to zinc deposition and adversely affects the kinetic performance of AZIBs. Researchers should pay more attention when conducting experiments involving the formation of an SEI.

3.2. Metal–ion additives

Metal–ion (M^{n+}) additives have been reported that they have the function of Zn dendrites growth inhibition. H^+ ions derived from solvated H_2O molecules obtain electrons from Zn to produce H_2, which then escapes from the electrolyte, with the by-product of OH^- in the electrolyte. These OH^- ions increase the pH at the anode surface, accelerate side reactions, and promote by-product formation. Unevenly distributed by-products accumulate and form protrusions. These protrusions have a strong electric field at their tip and attract more Zn^{2+}, further promoting dendrite growth. Metal–ion additives, which have negative reduction potential, can accumulate near the tips of the protrusions and prevent Zn protrusion formation. In LIB research, metal–ion additives with a reduction potential lower than that of Li^+, such as Cs^+ and Rb^+, were added to the electrolyte because they accumulated near the tips on the anode surface and inhibited dendrite formation through electrostatic shielding [84]. On the basis of this research, metal–ion additives with the same mechanism have been explored in ZIBs. For example, an electrolyte containing 1M Na_2SO_4 in 1M $ZnSO_4$ was employed in a zinc/sodium vanadate battery. The addition of Na^+ prevented the dissolution of sodium vanadate and inhibited Zn dendrite formation [85] (figure 11(a)). Hoang *et al* reported a gel electrolyte with added $PbSO_4$, which served as a corrosion inhibitor and dendrite growth suppressor [86]. The electrolyte containing $PbSO_4$ achieved a 20% lower Zn anode corrosion current density (figures 11(b) and (c)) and delivered higher capacity retention (300 cycles, 75% retention) than that of without Pb^{2+} (60% retention) (figure 11(d)). Wang *et al* added 0.1M $MgSO_4$ to 2M $ZnSO_4$ electrolyte [64]. In this electrolyte, the Zn^{2+} solvation sheath structure was altered by the

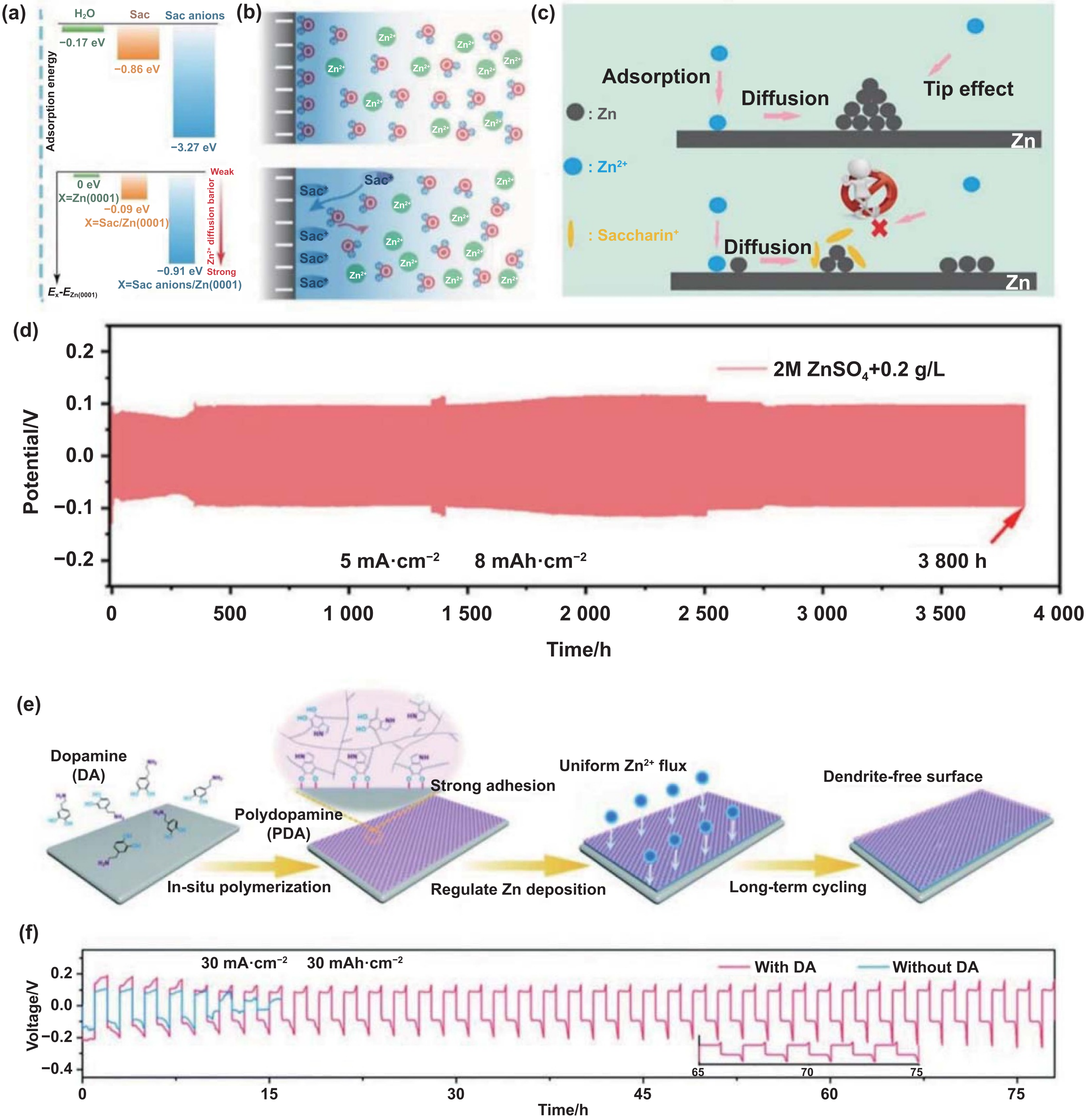

Figure 10. Figure of SEI/quasi-SEI formed electrolyte additives. (a) Adsorption energy of H_2O, Sac, and Sac anions on Zn (0001) lattice plane and the comparison of Zn^{2+} adsorption energy on the Zn (0001), Sac/Zn (0001), and Sac anions/Zn (0001) plane. [81] John Wiley & Sons. ©2021 Wiley-VCH GmbH. (b) Schematic descriptions of EDL structure with and without introducing Sac. [81] John Wiley & Sons. ©2021 Wiley-VCH GmbH. (c) Scheme of the Zn^{2+} diffusion and deposition processes on anode in 2 M $ZnSO_4$ electrolyte without (upper part) and with 0.20 $g \cdot l^{-1}$ saccharin sodium additive (lower part). Reprinted with permission from [82]. Copyright (2021) American Chemical Society. (d) Electrochemical performance of Zn/Zn symmetric cells in saccharin-containing electrolyte at 5 $mA \cdot cm^{-2}$ and 8 $mAh \cdot cm^{-2}$. Reprinted with permission from [82]. Copyright (2021) American Chemical Society. (e) Conceptual diagram of the in-situ formation of the multifunctional PDA SEI and its effective mechanism for dendrite-free Zn anode. Reproduced from [83] with permission from the Royal Society of Chemistry. (f) Galvanostatic cycling properties of Zn/Zn symmetric cells in the electrolytes with and without DA at 30 $mA \cdot cm^{-2}$, 30 $mAh \cdot cm^{-2}$. Reproduced from [83] with permission from the Royal Society of Chemistry.

additive Mg^{2+}, without electrochemical reduction on the Zn anode surface (figure 11(e)). DFT calculations demonstrated that Mg^{2+} was adsorbed onto the Zn anode. During deposition, the adsorbed Mg^{2+}, which had a highly negative reduction potential, accumulated around the Zn protuberances, forming an electrostatic shield. This shield prevented Zn^{2+} from

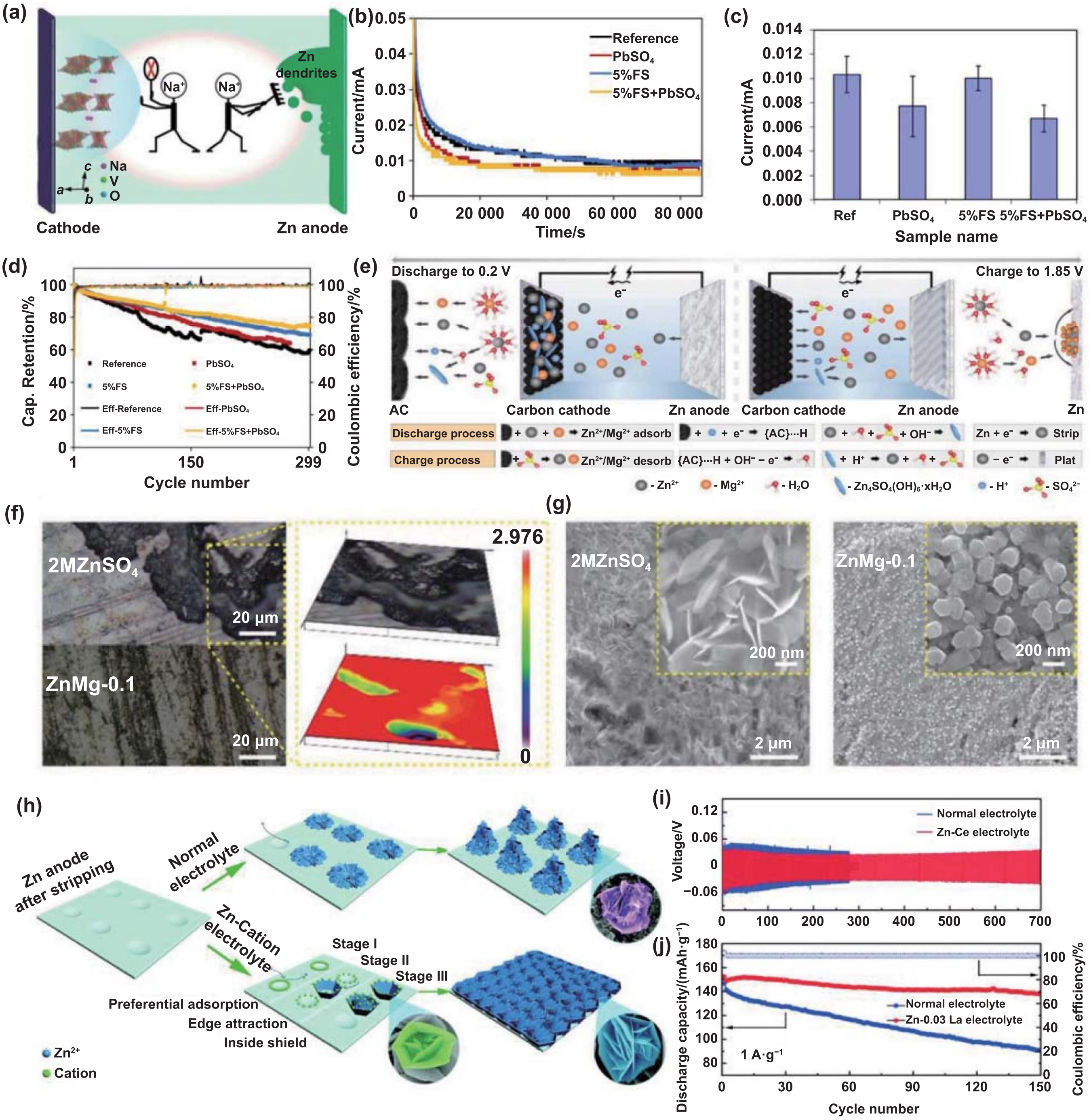

Figure 11. Figure of metal ions electrolyte additives. (a) Scheme of Na_2SO_4 additive suppresses the cathode dissolution and the formation of Zn dendrites. Float-charge current of batteries after 24 h monitoring. Reproduced from [85]. CC BY 4.0. (b) Representative data from single batteries. Reprinted from [86], © 2017 Elsevier Ltd. All rights reserved. (c) Statistical data from multiple batteries. Reprinted from [86], © 2017 Elsevier Ltd. All rights reserved. (d) Cycle performance and Coulomb efficiency of the batteries at 1 C. Reprinted from [86], © 2017 Elsevier Ltd. All rights reserved. (e) Schematic of AC//ZnMg-0.1//Zn energy storage devices. [64] John Wiley & Sons. ©2021 Wiley-VCH GmbH. (f) UTM optical images of Zn electrodes in the two electrolytes after 20 cycles and enlarged views. [64] John Wiley & Sons. ©2021 Wiley-VCH GmbH. (g) SEM images of Zn electrodes in the two electrolytes in the fully charged state after 20 cycles. [64] John Wiley & Sons. ©2021 Wiley-VCH GmbH. (h) Schematic diagram of the Zn deposition on the Zn foil after stripping in the normal and Zn–Ce electrolytes. Reproduced from [87] with permission from the Royal Society of Chemistry. (i) Cycling performance of Zn||Zn symmetric cells at 5 $mA \cdot cm^{-2}$, 1 $mAh \cdot cm^{-2}$. Reproduced from [87] with permission from the Royal Society of Chemistry. (j) Cycling performance comparison of the Zn||$NaV_3O_8 \cdot 1.5H_2O$ full cells using the electrolytes with and without 0.03 M $La_2(SO_4)_3$ at 1 $A \cdot g^{-1}$. Reproduced from [87] with permission from the Royal Society of Chemistry.

piling on the protrusions; instead, these ions were deposited on adjacent flat vacancies, leading to an even and regular deposition layer on the Zn anode (figure 11(e)). They employed a universal testing machine to observe the Zn anode surface, and the image showed that the Zn anode surface was smooth, and that the deposited Zn had assimilated with the Zn substrate (figure 11(f)). SEM images revealed that when the Mg^{2+} additive was used, the depositions on the Zn anode were preferentially orderly and dense rather than being flake-shaped, as commonly observed when using a pure $ZnSO_4$ electrolyte (figure 11(g)). These results proved that the Mg^{2+} additive, which was absorbed onto the Zn anode surface, could regulate the Zn^{2+} deposition microenvironment and inhibit parasitic reactions on the anode surface. Besides, Li *et al* introduced high valent cations, Ce^{3+} and La^{3+}, into the aqueous electrolyte as additives [87]. These added cations, priorly occupy the active sites on Zn anode and force the Zn^{2+} to deposit at other inert areas (figure 11(h)). Thus, the Zn||Zn symmetric cell with 2M $ZnSO_4$ + 0.01M $Ce_2(SO_4)_3$ show good cyclability of more than 700 h at 5 mA·cm^{-2}, 1 mAh·cm^{-2} (figure 11(i)). In their work, the electrolyte with La^{3+} cations additive also show better performance than pure $ZnSO_4$ electrolyte in Zn||$NaV_3O_8 \cdot 1.5H_2O$ full cell (figure 11(j)).

Metal cations with lower reduction potential than Zn^{2+} can strongly adsorb at the anode–electrolyte interface, forming a quasi-SEI layer. This type of interface layer can induce uniform Zn deposition and prevent Zn dendrite growth. Additionally, it can facilitate the desolvation of charge carriers and prevent the electrochemical contact of water molecules and the anode material, thus effectively mitigating the HER.

3.3. Polymer-type additives

Polymers have also been employed as electrolyte additives in ZIBs. Jin *et al* used polyethylene oxide (PEO) as a multifunctional additive to stabilize the Zn anode–electrolyte interface [65]. PEO interacted with Zn^{2+} through the ether functional group, suppressed the transfer kinetics of Zn^{2+}, and regulated the concentration of Zn^{2+} on the Zn anode (figure 12(a)), thereby promoting homogeneous Zn deposition. Additionally, the inert PEO molecules that were adsorbed onto the Zn anode protected the anode surface from H_2 generation, further stabilizing the anode–electrolyte interface. Yan *et al* also introduced PEO to their electrolyte in a different study. They discovered that adding PEO resulted in the cycle life of the ZIB increasing by a factor of 7–10 (figure 12(b)) and the coulomb efficiency also being significantly improved. They found that the PEO additive had different effects on two zinc salt solutions, $ZnSO_4$ and $Zn(TFSI)_2$ [88] (figure 12(c)). Zhou *et al* developed a polyaspartic acid additive [89] and discovered it had a strong ability to suppress dendrite growth and parasitic reactions (figure 12(d)). A Zn||Zn symmetric cell with the polyaspartic-containing electrolyte cycled for over 2000 times at 20 mA·cm^{-2} (figure 12(e)). Wu *et al* reported a kind of polymer additive sodium polystyrene sulfonate (PSS) in 1M $Zn(CF_3SO_3)_2$ electrolyte [90]. The added PSS would interact with H_2O through H–bonds and form a considerable polymer network, which could be a fast channel for Zn^{2+} transportation. Therefore, different from other polymer additives, Zn^{2+} shows good kinetic properties in electrolyte with PSS additive. Moreover, the PSS additive would also lay on the Zn anode surface to protect it from exposing to free H_2O, which suppresses the water decomposition and H_2 hydrogen. As a result, Zn||Zn symmetric cell with PSS additive achieved a high cycle life of 3000 h at 1 mAh·cm^{-2}, 1 mAh·cm^{-2} (figure 12(f)). Zhang *et al* proposed a novel additive strategy, they first fabricated a 3D Zn anode by combining Cu–Zn solid solution interface and zinc-oriented polyacrylamide electrolyte additive [91]. The result showed that the Cu–Zn shows great affinity to Zn^{2+}, and Zn^{2+} would selectively absorb on the acyl group of PAM and can be transferred along the polymer chains. Thus, dendrite-free Zn anode with homogeneous distribution of Zn^{2+} and uniform Zn nucleation is obtained (figure 12(g)). Therefore, the fabricated Zn||Zn symmetric cell has cycle for more than 280 h at a high areal capacity of 4 mAh·cm^{-2} (80% of discharge depth) (figure 12(h)). Peng *et al* reported a typical polymer additive polydiallyl dimethylammonium chloride (PDD) [92]. According to their report, the added PDD additive would not participate in the Zn^{2+} solvation sheath but distribute freely and absorb on Zn anode surface. The PDD polymer molecule would alter the electrical field distribution at the anode/electrolyte interface. Besides, the PDD additive also created a dual-function layer with outer positive charge rich layer and inner N-rich layer, further accelerating the Zn^{2+} desolvation and boosting the Zn^{2+} transportation kinetics (figure 12(i)). Moreover, owing to the dual function layer, water molecules are isolated from the Zn anode and dendrite-free Zn anode is obtained. They also found that the PDD additive can guide Zn^{2+} deposit along the (002) crystal plane. The assembled Zn||Zn symmetric cell exhibited a long life span of more than 3000 h at 1 mA·cm^{-2}, 1 mAh·cm^{-2}.

Usually, polymer additives work in two kinds of mechanisms. First, long chain polymer usually contains abundant functional groups, such as sulfur functional groups, acyl functional groups, amino functional groups, etc. These functional groups tend to show a strong affinity for Zn^{2+} ions. Zn^{2+} ions would combine with these functional groups and jump between them during transportation in the electrolyte, improving their transfer kinetics. At the same time, due to the relatively uniform distribution of functional groups in the electrolyte, when zinc ions are detached from the functional groups and deposited on the Zn anode, they will also be more uniformly distributed. Secondly, many polymer additives can also lay on Zn anode surface to form an artificial protective layer. This kind of adsorption layer can usually protect the Zn anode from interacting with active water molecules, thereby suppressing side reactions such as H_2O decomposition, hydrogen evolution, and corrosion, further prolonging the lifespan of Zn anode and batteries. In conclusion, these polymer additives show a solid ability to inhibit dendritic growth and side reactions and improve the AZIBs performance.

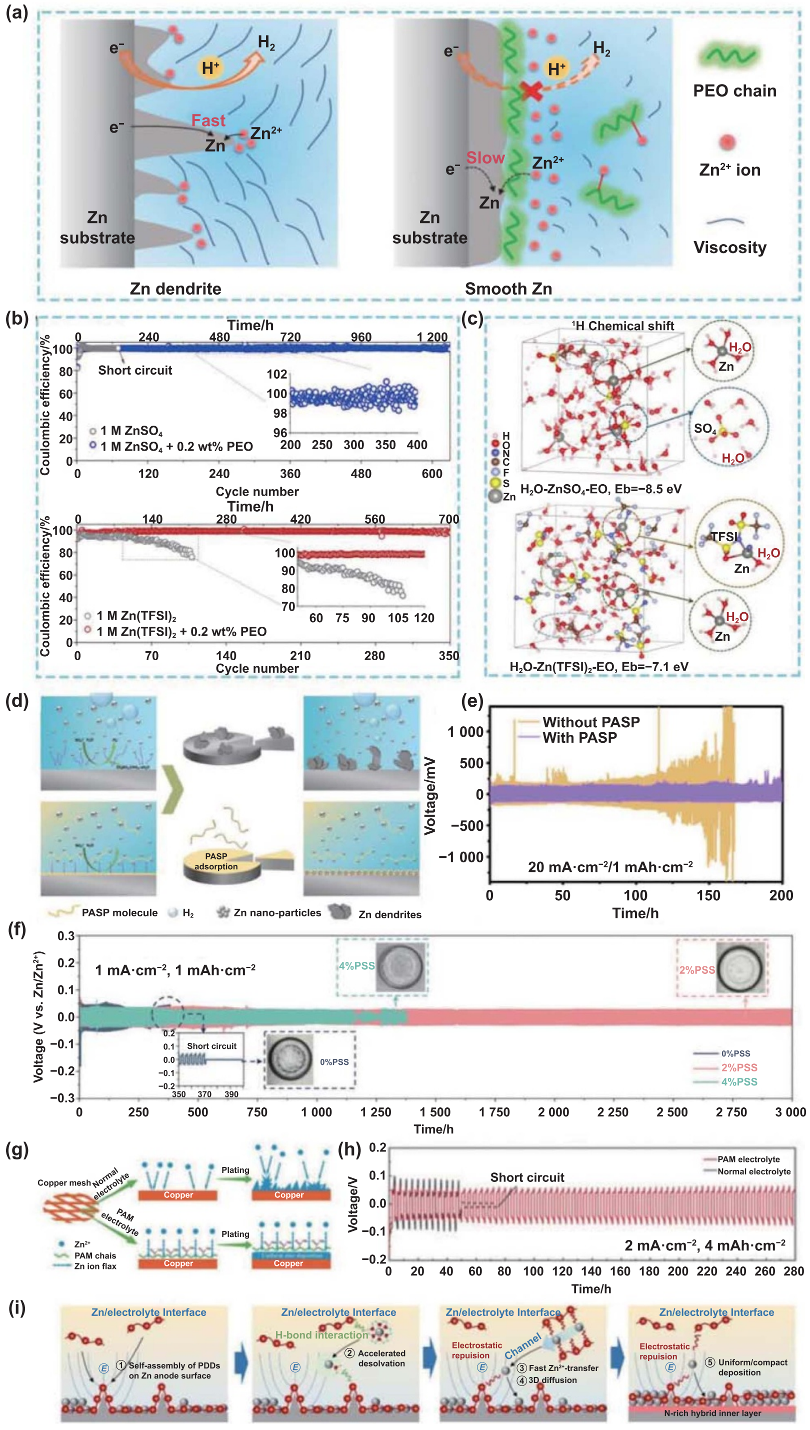

Figure 12. Figure of polymer-type electrolyte additives. (a) Schemes of Zn deposition behavior with and without PEO polymer additive, with dendritic growth and hydrogen evolution (left) and smooth Zn deposition and suppressed hydrogen generation (right). [65] John Wiley & Sons. ©2020 Wiley-VCH GmbH. (b) Cycling performance and Coulomb efficiency profiles of Zn anodes in $ZnSO_4$-based and $Zn(TFSI)_2$-based electrolytes with and without PEO additive. Reprinted from [88], © 2021 Elsevier Ltd. All rights reserved. (c) Snapshots of MD simulation for H_2O-$ZnSO_4$-EO and H_2O-$Zn(TFSI)_2$-EO, respectively, showing the Zn^{2+} environment in different electrolyte. Reprinted from [88], © 2021 Elsevier Ltd. All rights reserved. (d) Schemes of the Zn deposition behavior in the electrolyte without (upper part) and with (lower part) PASP additive. Reprinted from [89], © 2021 Elsevier B.V. All rights reserved. (e) Zn ‖ Zn symmetrical cells in the electrolyte with PASP additive cycle steadily at 20 mA·cm^{-2} and 1 mAh·cm^{-2}. Reprinted from [89], © 2021 Elsevier B.V. All rights reserved. (f) Cycle performance of Zn‖Zn symmetrical batteries with the 0%, the 2%, and the 4% PSS electrolytes at 1 mA·cm^{-2}, 1 mAh·cm^{-2}. [90] John Wiley & Sons. ©2023 Wiley-VCH GmbH. (g) Illustration of zinc deposition on the copper mesh in normal and PAM added electrolytes. [91] John Wiley & Sons. © 2019 WILEY-VCH Verlag GmbH & Co. KGaA, Wemheim. (h) Cycling performance in Zn‖Zn symmetric cells at 2 mA·cm^{-2}, 4 mAh·cm^{-2}. [91] John Wiley & Sons. © 2019 WILEY-VCH Verlag GmbH & Co. KGaA, Wemheim. (i) Schematic illustration of the Zn stripping/plating process in 1M $ZnSO_4$ + 2 wt% PDD electrolyte. [92] John Wiley & Sons. © 2023 Wiley-VCH GmbH.

3.4. Adsorption-type additives

Adsorption-type additives usually have strong affinity for the zinc metal anode. The additive molecules tend to be adsorbed onto the anode, occupy active sites where water would otherwise be adsorbed, and form a special interface layer, thereby preventing water decomposition, inhibiting hydrogen evolution, and hindering side reactions.

Chen *et al* added arginine, a cationic surfactant electrolyte additive, to the electrolyte [93]. The arginine molecules were hydrolyzed into arginine cations (Arg^+), which were preferentially adsorbed onto zinc protuberances during zinc plating due to the accumulation effect of charges at the tip (figure 13(a)). Arg^+ also increased the Zn nucleation overpotential, suppressed irregular nonplanar dendrite growth, and led to uniform Zn deposition. As a result, the Zn||Cu asymmetric cell showed high average CE of 99.47% after 850 long cycles at 0.5 $mA \cdot cm^{-2}$, 0.1 $mAh \cdot cm^{-2}$. Bayaguud *et al* reported the use of an extremely low concentration of the cationic electrolyte additive tetrabutylammonium sulfate, which was electrostatically adsorbed onto and accumulated near Zn protrusions, forming a cation-containing quasi-SEI protective layer during the plating process and thus inducing the uniform deposition of zinc [94] (figure 13(b)). Surprisingly, the Zn||Zn symmetric cells exhibited good cycle stability of more than 160 h at 5 $mA \cdot cm^{-2}$, 5 $mAh \cdot cm^{-2}$. Sun *et al* employed glucose, a low-cost additive, to modify the structure of their aqueous electrolyte, with the aim of promoting Zn stripping-plating behavior and boosting electrochemical performance [35]. They found that glucose molecules substituted one water molecule in the $Zn(H_2O)_6{}^{2+}$ solvent sheath, altering the solvation structure (figure 13(c)) and thereby hindering H_2O decomposition on the anode and the resulting parasitic reactions. Additionally, glucose was preferentially adsorbed onto the Zn anode surface, preventing disordered Zn^{2+} distribution and nucleation and further suppressing dendrite growth. Consequently, the Zn||Zn symmetric cells with glucose additive show excellent cycling stability of up to 270 h at 5 $mA \cdot cm^{-2}$ with 5 $mAh \cdot cm^{-2}$.

Zhang *et al* proposed a simple method for introducing ethylenediaminetetraacetic acid disodium salt into $ZnSO_4$ and found that this additive simultaneously suppressed dendritic zinc deposition and hydrogen evolution [95]. They suggested that $EDTA^{4-}$ anions were adsorbed onto the anode surface, occupying active sites where H_2 could be generated and prevent water decomposition (figure 13(d)). The added EDTA also promoted Zn^{2+} desolvation by removing H_2O from the $Zn(H_2O)_6{}^{2+}$ solvation structure. Qiao *et al* revealed that the electrochemical performance of the cell was considerably improved by the additive, and they discovered high reversibility and the high coulomb efficiency of 99.5% for 700 cycles (figure 13(e)).

Xu *et al* employed trace amount (2 vol%) of diethyl ether (Et_2O) as an electrolyte additive [96] and discovered that it significantly improved the performance of Zn-MnO_2 full cell. The Et_2O molecules were preferentially adsorbed onto protuberances, meaning that Zn^{2+} were forced to nucleate in a nearby area, which led to the formation of a uniform Zn anode surface. The assembled Zn-MnO_2 coin cell had a long lifespan of over 4000 cycles with 97.7% capacity retention (figure 13(f)).

In addition to the additives mentioned in this section, the above-mentioned $BMIM^+$ additive, sodium PSS, PDD could also be absorbed on the surface of Zn anode. These additives can also be categorized into adsorption-type additives. Moreover, additives such as $BMIM^+$ and PDD also have a texture effect on Zn deposition. The details are discussed in sections 2.2, 3.3, and 4.1.

The absorption-type additives discussed in this subsection mainly work by adsorbing onto the Zn anode surface through physical adsorption, forming a quasi-SEI. This kind of protective layer can effectively isolate H_2O and Zn anode from directly contacting, guide uniform Zn deposition, and suppress the parasite reactions.

4. Other positive effects of additives on AZIB performance

4.1. Texture effect on Zn anode

The texture effect of electrolyte additives plays a vital role in the optimization of Zn anodes. This effect of additives regulates the anode's crystal planes onto which zinc ions are deposited. For a pure $ZnSO_4$ electrolyte, Zn^{2+} is deposited on the (100) crystal plane of the Zn anode. This type of deposition tends to lead to the uneven accumulation of Zn^{2+}. These accumulated Zn^{2+} ions undergo reduction and form Zn protrusions, which induce the dendrites growth that pierce the separator, resulting in battery short circuit. Generally, electrolyte additives transform the Zn deposition crystal plane from (100) to (002) and (103). Zn^{2+} exhibits ordered deposition behavior on the latter two crystal planes. Therefore, more regular, uniform, and dense zinc deposition can be achieved if this deposition occurs on the (002) and (103) crystal planes. This would lead to a long-cycle, stable zinc negative electrode and improved battery life.

Wei *et al* employed 1,4-dioxane (DX) as an additive in the $ZnSO_4$ electrolyte and discovered that the texture effect of the additive optimized electrochemical performance [97]. The added DX molecules were absorbed onto the Zn anode surface, constructing an artificial SEI layer that inhibited harmful side reactions. The additive preferentially adsorbed on the (002) crystal surface of the Zn anode and thus prevented contact between water and the (002) crystal plane. Instead, the (002) crystal plane was exposed to Zn^{2+}, facilitating Zn^{2+} deposition and growth along the aforementioned plane. Regular deposition was achieved, and the anode was dendrite-free. The Zn||Zn symmetric cell could be cycled for 1000 h at 10 $mA \cdot cm^{-2}$, 10 $mAh \cdot cm^{-2}$, as illustrated in figures 14(a) and (b). In addition, when the DX additive was used, zinc was more likely to be deposited on the (002) crystal plane (figure 14(c)).

Sun *et al* investigated the texture effect of indium sulfate, tin oxide, and boric acid additives [57]. They employed x-ray diffraction to characterize the Zn synthesized when using

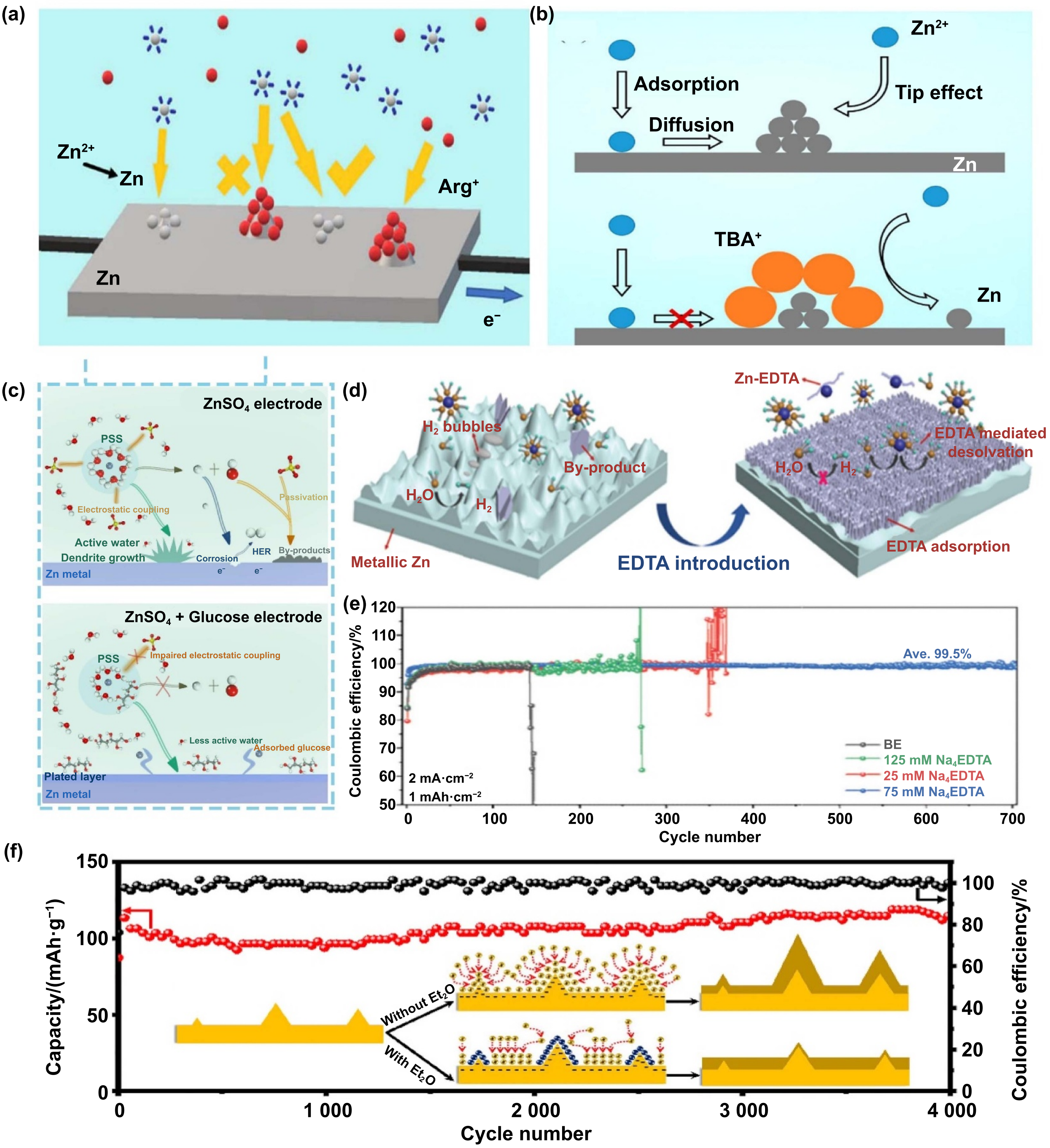

Figure 13. Figure of adsorption-type electrolyte additives. (a) Conceptual description of arginine cations inhibits the charge accumulation on Zn anode and prevents dendrites growth. Reprinted with permission from [93]. Copyright (2021) American Chemical Society. (b) Schemes of the Zn^{2+} diffusion and deposition behavior on Zn anode in electrolytes without (top part) and with TBA_2SO_4 additive (bottom part). Reprinted with permission from [94]. Copyright (2020) American Chemical Society. (c) Schemes of different reaction processes of Zn^{2+} solvation structure and corresponding interfacial interaction of Zn anode/electrolyte interface in pure $ZnSO_4$ electrolyte and glucose-containing electrolyte. [35] John Wiley & Sons. ©2021 Wiley-VCH GmbH. (d) Schematic of Zn/electrolyte interphase behaviors during Zn plating in $ZnSO_4$ electrolyte and EDTA-functionalized $ZnSO_4$ electrolyte. [95] John Wiley & Sons. ©2021 Wiley-VCH GmbH. (e) Coulomb efficiency of Cu//Zn cells in electrolytes with/without Na_4EDTA at 2 mA·cm^{-2}, 1 mAh·cm^{-2}. [95] John Wiley & Sons. ©2021 Wiley-VCH GmbH. (f) Schemes of Zn deposition morphology evolution in traditional aqueous electrolyte with and without Et_2O additive; and high-rate electrochemical performance of Zn/MnO_2 battery in electrolyte with Et_2O additive. Reprinted from [96], © 2019 Elsevier Ltd. All rights reserved.

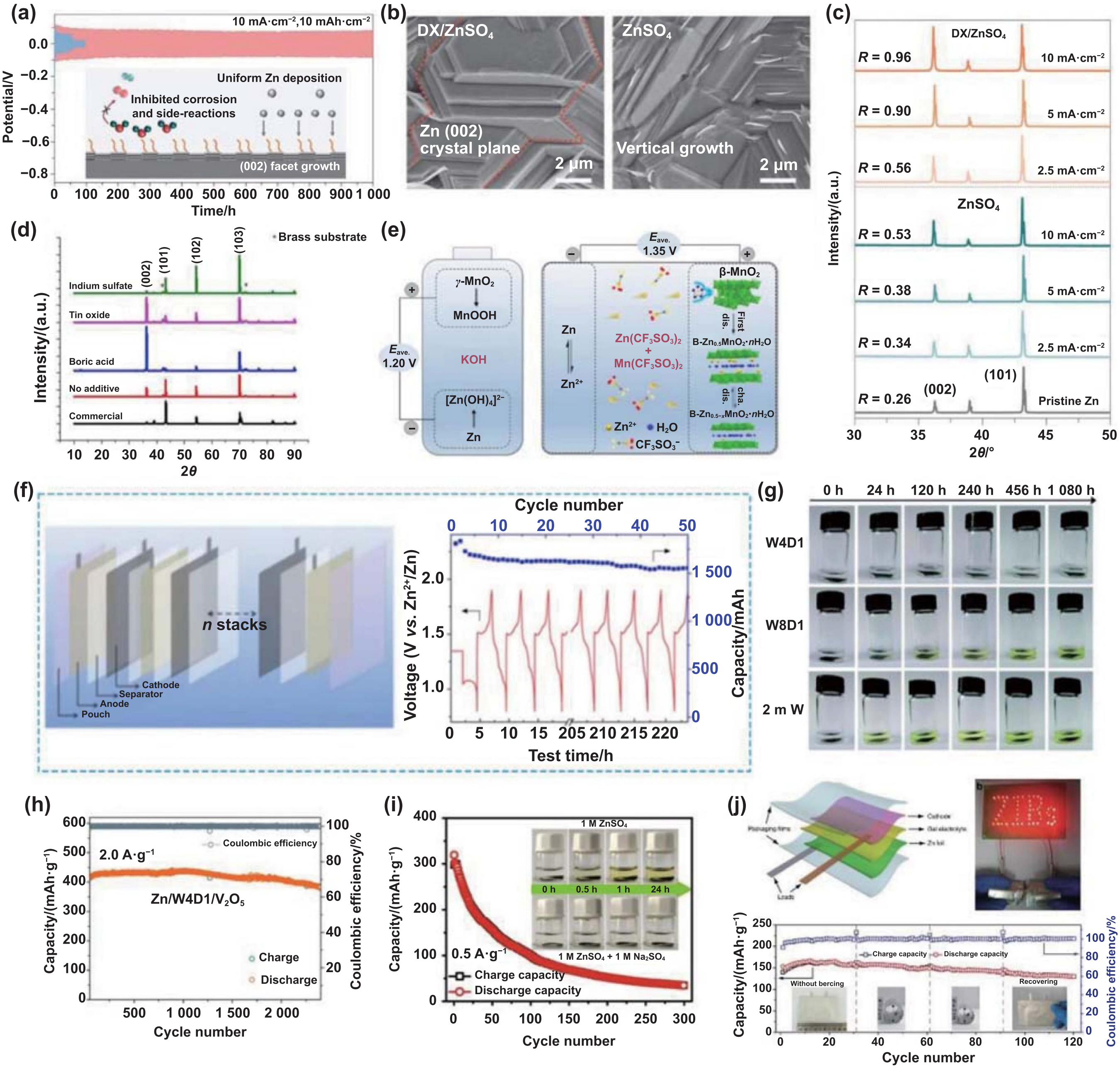

Figure 14. Figure of other effect from electrolyte additives. (a) Schematic mechanism of 1,4-dioxane inducing Zn^{2+} deposition orientation and Zn||Zn symmetric cell cycle performance. Reprinted with permission from [97]. Copyright (2023) American Chemical Society. (b) SEM image of Zn deposition orientation with 1,4-dioxane additive. Reprinted with permission from [97]. Copyright (2023) American Chemical Society. (c) XRD comparison of deposited Zn crystal plane with and without 1,4-dioxane at different current density. Reprinted with permission from [97]. Copyright (2023) American Chemical Society. (d) XRD comparison of deposited Zn crystal plane with and without boric acid, tin oxide, indium sulfate. [57] John Wiley & Sons. © 2018 WILEY-VCH Verlag GmbH & Co. KGaA, Wemheim. (e) Schematic diagram of $Mn(CF_3SO_3)_2$ additive suppressing MnO_2 dissolution. Reproduced from [98]. CC BY 4.0. (f) Pouch cell stacking diagram and cycle performance. Reproduced from [98]. CC BY 4.0. (g) Optical images of V_2O_5 electrodes immersed in W4D1, W8D1, and 2 m W solutions for different periods. Reproduced with permission from [74]. © 2021 The Author(s). Published by the Royal Society of Chemistry, CC BY-NC 3.0. (h) Cycle performance of Zn/W4D1/V_2O_5 full cell. Reproduced with permission from [74]. © 2021 The Author(s). Published by the Royal Society of Chemistry, CC BY-NC 3.0. (i) Cycling performance Zn||NVO full cell in $ZnSO_4$ electrolyte and optical images of NVO electrodes in electrolytes with and without Na_2SO_4 additive for different periods. Reproduced from [85]. CC BY 4.0. (j) Cycling performance under different bending states of the flexible quasi-solid-state Zn||NVO battery with $ZnSO_4$ + Na_2SO_4 electrolyte. Reproduced from [85]. CC BY 4.0.

electrolytes containing the aforementioned additives. The results revealed that these additives led to zinc deposition preferentially on the (002) and (103) crystal planes, as shown in figure 14(d). According to Chen *et al*, Zn deposits along these crystal orientations exhibited great resistance to disordered nucleation and dendrite growth. Additionally, the corrosion current during the stripping–plating process was much smaller (∼11 times smaller) when those additives were employed, indicating excellent corrosion resistance. In addition to these substances, DMSO was used as an additive to regulate the orientation of Zn deposition because it has lower adsorption energy on the (002) crystal plane. The details are provided in section 2.1. Besides, BMIM+ additive employed by Huang *et al* (section 2.2) can also regulate the Zn deposition crystal plane. Huang *et al* found that $BMIm^+$ cations would priorly be absorbed on the (100) and (001) crystal plane of Zn and occupied the deposition sites, forcing the Zn^{2+} to deposit along the (002) crystal plane. The battery performance with BMIM+ additives was surprisingly improved. Moreover, Peng *et al* found that PDD [92] could also induce Zn deposition order. Different from other additives that are preferentially absorbed on the (100) and (001) plane, PDD additive would form a unique artificial function layer, which could protect the Zn anode from an active free water molecule and guide the Zn^{2+} deposit along (002) crystal plane. The battery with PDD additive also performs better than those with blank electrolytes (section 3.3).

4.2. Additives for suppressing cathode dissolution

In addition to having a texture effect on the anode in a cell, some metal–ion additives exert effects on the cathode. Manganese dioxide and vanadium oxide, the two most commonly used cathode materials for AZIBs, dissolve easily in the electrolyte [99–102]. Cathode dissolution reduces the utilization of active materials and leads to irreversible capacity loss, which shortens the cycle lifespan of AZIBs and results in poor electrochemical performance. Therefore, suppressing cathode dissolution has become crucial. Researchers have found that an electrolyte additive that comprises a metal salt with the same cation as the cathode material can increase the concentration of cations in the electrolyte and regulate the dissolution balance, thereby inhibiting the reverse reaction and preventing the dissolution of the cathode material.

4.2.1. Manganese dioxide dissolution. Manganese dioxide dissolution in AZIBs is a phenomenon that cannot be ignored [103]. In a mildly acidic $ZnSO_4$ electrolyte, the valence of manganese cations changes from +4 to +3 during operation of AZIBs [104, 105]. However, Mn^{3+} cations cannot stably exist in the electrolyte and are prone to the disproportionation reaction [106]. Mn^{3+} is disproportionated into Mn^{4+} and Mn^{2+} cations [12]. Thus, soluble Mn^{2+} cations are produced, which in turn leads to the disruption of the MnO_2 structure and thus dissolution of the cathode [107]. Pan *et al* were the first to propose adding $MnSO_4$ to the $ZnSO_4$ electrolyte to inhibit the dissolution of MnO_2 [12]. Their Zn||MnO_2 cells had up to 92% capacity retention after 5000 cycles and excellent rate performance. Zhang *et al* added 0.1M $Mn(CF_3SO_3)_2$–3M $Zn(CF_3SO_3)_2$ electrolyte to form 3M $Zn(CF_3SO_3)_2$ + 0.1M $Mn(CF_3SO_3)_2$ mixed electrolyte [98]. The addition of $Mn(CF_3SO_3)_2$ led to the formation of a protective layer on the surface of MnO_2 during cycling and inhibited cathode dissolution (figure 14(e)), thus extending the battery's cycle life and improving its performance. By stacking electrodes together in a pouch battery, they obtained high capacity of 1550 mAh, as illustrated in figure 14(f).

4.2.2. Vanadium oxide dissolution. Similar to the case of manganese dioxide, vanadium oxide commonly dissolves in a weakly acidic $ZnSO_4$ electrolyte and in the $Zn(CF_3SO_3)_2$ electrolyte [108, 109]. Although the solubility of vanadium oxide in electrolytes is very low, as the number of cycles increases, a large number of vanadium cations with different valence states are generated near the cathode, and these ions are soluble in the electrolyte; vanadium oxide dissolution thus occurs [110]. Dong *et al* immersed several V_2O_5 electrodes in three electrolytes-2M $Zn(CF_3SO_3)_2$ electrolyte, W4D1 (water:DMC molecular ratio = 4:1), and W8D1 (water:DMC molecular ratio = 8:1)-and investigated the electrodes' dissolution. After immersion for 24 h, the 2 M $Zn(CF_3SO_3)_2$ and W8D1 electrolytes turned light yellow, and over time, they turned yellow-green; the optical images are presented in figure 14(g) [74]. This result indicated severe V_2O_5 dissolution. By contrast, the W4D1 electrolyte remained transparent even after the electrodes had been immersed in it for 1080 h. A full cell containing W4D1 exhibited favorable capacity retention after cycling for 1000 h (figure 14(h)). Using an organic solvent as an electrolyte additive to reduce the solubility of the cathode material in the electrolyte is a promising strategy for inhibiting cathode dissolution. Common ion salt additives are also effective for inhibiting vanadium oxide dissolution. Wan *et al* [85] synthesized NaV_3O_8 (NVO) by embedding Na^+ into V_2O_5, and they assembled a full cell with Zn foil and a NVO cathode. They also added Na_2SO_4 to the $ZnSO_4$ electrolyte. The added Na_2SO_4 deionized the Na^+ ions in the electrolyte, which altered the dissolution balance of Na^+ in the electrolyte; thus, NVO cathode dissolution was successfully suppressed. They also conducted dissolution testing by immersing an NVO electrode in a pure $ZnSO_4$ electrolyte and $ZnSO_4$ + Na_2SO_4 electrolyte to make a comparison. Adding Na_2SO_4 to the electrolyte effectively suppressed NVO dissolution. The optical images are shown in figure 14(i). Furthermore, the additive improved the cycle stability of the full cell and promoted the electrochemical performance of the cell. The assembled pouch battery was successfully cycled for more than 120 cycles (figure 14(j)).

4.3. Extended operating temperature

Traditional aqueous electrolyte employed in AZIBs has the problems of high freezing point, low ionic conductivity at low temperature, and severe side reactions at high temperature, which significantly limits their operation in extreme environments [111, 112]. Therefore, expanding the operating temperature window of AZIBs has also attracted widespread attention. Generally speaking, hydrogen bonds between water molecules affect the freezing point of aqueous electrolytes [113]. Therefore, introducing hydrogen bond acceptors into the electrolytes to break the hydrogen bonds network can effectively lower the freezing point of aqueous electrolytes [114]. Therefore, some organic additives, such as DMSO, EG, etc, are widely used since they cannot only interact with H_2O and break the original hydrogen bond network, adjust the Zn^{2+} solvation structure, and improve the AZIB's performance [48]. As mentioned above, Feng *et al* introduced DMSO into the electrolyte as an effective additive [66]. Owing to the stronger HBs between DMSO and H_2O molecules, the ion conductivity at the low temperature of −20 °C is significantly improved. Consequently, the Zn||MnO_2 cell exhibited excellent long cycling stability for over 3000 cycles even at 10C under 20 °C and more than 300 cycles at 1C under −20 °C (figures 4(d) and (e)). Hao *et al* added methanol into the $ZnSO_4$ electrolyte [70]. With the addition of methanol, hydrogen bonds between water molecules were broken, and dendrite-free Zn deposition was achieved. Besides, the methanol added interacts with water and reduces the activity of free water molecule, further suppressing the H_2 evolution and Zn anode corrosion under both moderate and high temperature. Therefore, the Zn metal anode in Zn||Cu asymmetric cell shows high reversibility of an average CE of 98.7% and 98.1% at −20 °C and 60 °C, respectively, with 50% methanol additive. Qin *et al* introduced EG as an additive. The result revealed that the electrolytes containing 32 vol%−68 vol% EG remain liquid even at −50 °C [71]. They also found that as the EG content increased to 40%vol and 68%vol, the Zn||Zn symmetric cell remained stable at −10 °C and −20 °C, respectively, while the electrolyte with no EG additive or only 10%vol EG polarized suddenly and failed at −10 °C (figure 6(e)). The result indicates that EG could be an outstanding anti-freezing solvent used in AZIBs electrolyte.

In brief, the key point to extend the operating temperature range of AZIBs through electrolyte additives is to break the hydrogen bonds network and suppress the side reactions on the Zn anode. The former can lower the electrolyte's freezing point so that zinc batteries can operate at lower temperatures. The latter protects the zinc anode from severe side reactions under high temperatures. Therefore, organic solvents containing hydrogen bond acceptors are widely investigated by researchers. Some industrial antifreeze agents, including methanol, EG, isopropanol, glycerin etc., show miraculous effects in AZIBs electrolyte antifreeze. At the same time, since most of these substances can limit the activity of free water in the electrolyte, they can usually inhibit side reactions at high temperatures and protect the Zn anode. In addition, some other organic compounds, such as sulfones and ethers, may also be good choices, which need to be further developed by researchers.

4.4. Safety issues associated with additives

Additives also affect the safety performance of AZIBs [34, 115]. Unlike LIBs, AZIBs are completely safe and nontoxic because they contain a water-based electrolyte [36, 116, 117]. However, the additives introduced by researchers may affect these beneficial characteristics [118, 119]. When used as additives, the organic solvents discussed in this review—DMC, DMSO, methanol, DX, and others [59, 70, 72, 74, 97]—increase the flammability and toxicity of the electrolyte due to their low ignition point and toxicity. Therefore, when screening organic additives, researchers should consider the impact of these additives on the flammability of an aqueous electrolyte. Additionally, some salts containing heavy metal ions (such as Pb and Cr) should be used with caution. Pb^{2+} ions in additives can be adsorbed onto the surface of zinc ions during cycling [86], changing the crystal plane orientation of Zn^{2+} deposition on the anode to improve battery performance. However, heavy metal ions such as Pb^{2+} are toxic and can thus have negative effects on the environment when a battery is discarded. They also increase the cost of recycling a battery.

Herein, we make two suggestions:

First, when any organic additive is included in the electrolyte, a flammability test should be conducted on the electrolyte. Such tests are very common in research on LIBs [84, 120] and should also be performed in research on ZIB electrolytes.

Second, salts and substances containing heavy metal ions should be avoided. AZIBs should be kept environmentally friendly and nontoxic [121, 122].

5. Summary and outlook

AZIBs are regarded as promising energy storage devices due to their high specific volume capacity, absolute safety, and many other advantages [123]. They are expected to be applied for large-scale energy storage in the future to fill a gap that LIBs cannot. Nevertheless, many problems remain. In this review, utilizing electrolyte additives to address potential problems with ZIBs—including Zn dendrite growth, hydrogen evolution on and corrosion of Zn anodes, and cathode material dissolution and disruption of the cathode structure—has been discussed, and the mechanisms underlying the action of these additives have also been introduced from the perspective of solvation. The strategies proposed by researchers are worthy of further development and reference in future work. Although introducing additives in the electrolyte in an AZIB has achieved satisfactory results, more attention should be paid to solving problems such as low electrochemical stability, incompatibility of additives with anodes and cathodes, poor ionic conductivity, and high nucleation overpotential caused by the additives.

Two categories of aqueous additives have been summarized in this review: additives optimizing the solvation sheath structure and additives promoting the formation of an SEI or quasi-SEI layer. Some organic additives, such as DMC and DME, are associated with safety hazards for AZIBs, causing an aqueous electrolyte that was absolutely safe to become less safe. This problem should also be considered when developing organic additives to ensure higher electrochemical performance. For each type of additive, there must exist a critical point at which a reasonable balance is achieved between electrochemical performance and safety. At this point, additives can be more widely applied in electrolytes.

Regarding dipole organic additives, one strategy is to examine small-molecule additives. As mentioned in the earlier text, most reported organic additives are macromolecular organic additives, and their size has led to steric hindrance of Zn^{2+} transport in the electrolyte, resulting in poor Zn^{2+} transfer kinetics. By contrast, small-molecule additives can attack the Zn^{2+} solvent sheath and limit the activity of free water, and they negatively affect Zn^{2+} transfer kinetics to a lower degree, thus ensuring rapid Zn^{2+} transport kinetics and improving electrochemical performance.

Ionic liquid additives, which usually have high viscosity, tend to reduce the ionic conductivity of the electrolyte. In addition, most ionic liquids are stable within a wide voltage window. Therefore, broadening the voltage window can also be considered an advantage when developing ionic liquid additives. Ionic liquids with wider voltage windows have larger molecular structures and higher viscosity. Therefore, balancing the relationship between viscosity, ionic conductivity, and voltage window is crucial.

Polymer additives often exhibit low electrical conductivity and are even insulating. To some extent, when these substances are adsorbed onto the surface of a Zn anode, they limit the interaction of Zn^{2+} with electrons, causing a large overpotential for Zn^{2+} nucleation. Therefore, when polymers are employed as additives, these shortcomings should be reasonably addressed.

Similar to polymer additives, SEI-constructing and adsorption-type additives also result in a large overpotential for Zn nucleation and poor Zn^{2+} transfer kinetics at the electrolyte/anode interface. The introduction of different ions into an aqueous electrolyte also causes uncertainty. Furthermore, cost and safety must be accounted for when applying polymer additives.

The Zn^{2+} desolvation energy barrier should also be considered when introducing additives, and this aspect has been ignored in much related research. An old Chinese saying states the following: 'solving one problem causes another to crop up.' By replacing water molecules in the solvent sheath, additive molecules often lead to a large Zn^{2+} desolvation energy barrier; one problem has been solved, but another has been created. Fourier transform infrared spectroscopy, Raman spectroscopy, and x-ray absorption fine structure spectroscopy should be combined to characterize the solvation structure and calculate the coordination number of additives in the Zn^{2+} solvent sheath. Such techniques can reveal the solvation structure and enable the calculation of the Zn^{2+} desolvation energy for that solvation structure, and the findings can indicate the optimal type and amount of additive.

In previous work, scholars have mostly aimed to discover additives that improve the performance of Zn anodes. Whether the additives have any adverse effects on the cathode has not yet been systematically investigated. For instance, Mn^{2+} is well-known to suppress the dissolution of MnO_2. However, the possible negative effects of additives on the kinetic intercalation–deintercalation behavior of Zn^{2+} and structural stability of cathode materials should also be explored.

Finally, it should be noted that an additive is not the only way to solve the problems with ZIBs. An additive could be combined with various other solutions (such as a multisalt electrolyte, eutectic electrolyte, or quasi-solid electrolyte) to design novel electrolytes. Such combinations would require the consideration of numerous parameters such as solubility, pH, chemical stability, ionic conductivity, viscosity, and cost but may also be an effective way for improving overall battery performance.

Conflict of interest

We declare no competing interests.

ORCID iD

Chunyi Zhi https://orcid.org/0000-0001-6766-5953

References

[1] Lin D C, Liu Y Y and Cui Y 2017 Reviving the lithium metal anode for high-energy batteries *Nat. Nanotechnol.* **12** 194–206

[2] Liu K, Liu Y Y, Lin D C, Pei A L and Cui Y 2018 Materials for lithium-ion battery safety *Sci. Adv.* **4** eaas9820

[3] Hou Y, Huang Z D, Chen Z, Li X L, Chen A, Li P, Wang Y B and Zhi C Y 2022 Bifunctional separators design for safe lithium-ion batteries: suppressed lithium dendrites and fire retardance *Nano Energy* **97** 107204

[4] Xu K 2004 Nonaqueous liquid electrolytes for lithium-based rechargeable batteries *Chem. Rev.* **104** 4303–418

[5] Borodin O *et al* 2017 Liquid structure with Nano-heterogeneity promotes cationic transport in concentrated electrolytes *ACS Nano* **11** 10462–71

[6] Wang F, Borodin O, Gao T, Fan X L, Sun W, Han F D, Faraone A, Dura J A, Xu K and Wang C S 2018 Highly reversible zinc metal anode for aqueous batteries *Nat. Mater.* **17** 543–9

[7] Li M, Wang C S, Chen Z W, Xu K and Lu J 2020 New concepts in electrolytes *Chem. Rev.* **120** 6783–819

[8] Liu C X, Xie X S, Lu B G, Zhou J and Liang S Q 2021 Electrolyte strategies toward better zinc-ion batteries *ACS Energy Lett.* **6** 1015–33

[9] Pei Z X 2022 Symmetric is nonidentical: operation history matters for Zn metal anode *Nano Res. Energy* **1** 9120023

[10] Li Q, Chen A, Wang D H, Zhao Y W, Wang X Q, Jin X, Xiong B and Zhi C Y 2022 Tailoring the metal electrode morphology via electrochemical protocol optimization for long-lasting aqueous zinc batteries *Nat. Commun.* **13** 3699

[11] Song M, Tan H, Chao D L and Fan H J 2018 Recent advances in Zn-Ion batteries *Adv. Funct. Mater.* **28** 1802564

[12] Pan H L *et al* 2016 Reversible aqueous zinc/manganese oxide energy storage from conversion reactions *Nat. Energy* **1** 16039

[13] Zheng X H, Ahmad T and Chen W 2021 Challenges and strategies on Zn electrodeposition for stable Zn-ion batteries *Energy Storage Mater.* **39** 365–94

[14] Xu Y, Zheng X H, Sun J F, Wang W P, Wang M M, Yuan Y, Chuai M, Chen N, Hu H L and Chen W 2022 Nucleophilic interfacial layer enables stable Zn anodes for aqueous Zn batteries *Nano Lett.* **22** 3298–306

[15] Blanc L E, Kundu D and Nazar L F 2020 Scientific challenges for the implementation of Zn-Ion batteries *Joule* **4** 771–99

[16] Goodenough J B and Kim Y 2010 Challenges for rechargeable Li batteries *Chem. Mater.* **22** 587–603

[17] Kundu D, Hosseini Vajargah S, Wan L W, Adams B, Prendergast D and Nazar L F 2018 Aqueous *vs.* nonaqueous Zn-ion batteries: consequences of the

desolvation penalty at the interface *Energy Environ. Sci.* **11** 881–92
[18] Goodenough J B and Park K-S 2013 The Li-ion rechargeable battery: a perspective *J. Am. Chem. Soc.* **135** 1167–76
[19] Goodenough J B 2014 Electrochemical energy storage in a sustainable modern society *Energy Environ. Sci.* **7** 14–18
[20] Zhang R, Wu Z X, Huang Z D, Guo Y, Zhang S C, Zhao Y W and Zhi C Y 2023 Recent advances for Zn-gas batteries beyond Zn-air/oxygen battery *Chin. Chem. Lett.* **34** 107600
[21] Zhao Y W *et al* 2022 Few-layer bismuth selenide cathode for low-temperature quasi-solid-state aqueous zinc metal batteries *Nat. Commun.* **13** 752
[22] Liang G J *et al* 2023 Development of rechargeable high-energy hybrid zinc-iodine aqueous batteries exploiting reversible chlorine-based redox reaction *Nat. Commun.* **14** 1856
[23] Yang S, Guo X, Lv H M, Han C P, Chen A, Tang Z J, Li X L, Zhi C Y and Li H F 2022 Rechargeable iodine batteries: fundamentals, advances, and perspectives *ACS Nano* **16** 13554–72
[24] Li Q, Wang D H, Yan B X, Zhao Y W, Fan J and Zhi C Y 2022 Dendrite issues for zinc anodes in a flexible cell configuration for zinc-based wearable energy-storage devices *Angew. Chem., Int. Ed.* **61** e202202780
[25] Cui H L *et al* 2022 High-voltage organic cathodes for zinc-ion batteries through electron cloud and solvation structure regulation *Angew. Chem., Int. Ed.* **61** e202203453
[26] Liang G J, Mo F N, Li H F, Tang Z J, Liu Z X, Wang D H, Yang Q, Ma L T and Zhi C Y 2019 A universal principle to design reversible aqueous batteries based on deposition–dissolution mechanism *Adv. Energy Mater.* **9** 1901838
[27] Jiang L W, Dong D J and Lu Y-C 2022 Design strategies for low temperature aqueous electrolytes *Nano Res. Energy* **1** 9120003
[28] Xie F X, Li H, Wang X S, Zhi X, Chao D L, Davey K and Qiao S-Z 2021 Mechanism for zincophilic sites on zinc-metal anode hosts in aqueous batteries *Adv. Energy Mater.* **11** 2003419
[29] Wu K, Huang J H, Yi J, Liu X Y, Liu Y Y, Wang Y G, Zhang J J and Xia Y Y 2020 Recent advances in polymer electrolytes for zinc ion batteries: mechanisms, properties, and perspectives *Adv. Energy Mater.* **10** 1903977
[30] Bayaguud A, Fu Y P and Zhu C B 2022 Interfacial parasitic reactions of zinc anodes in zinc ion batteries: underestimated corrosion and hydrogen evolution reactions and their suppression strategies *J. Energy Chem.* **64** 246–62
[31] Xie J, Liang Z J and Lu Y-C 2020 Molecular crowding electrolytes for high-voltage aqueous batteries *Nat. Mater.* **19** 1006–11
[32] Suo L M, Borodin O, Gao T, Olguin M, Ho J, Fan X L, Luo C, Wang C S and Xu K 2015 "Water-in-salt" electrolyte enables high-voltage aqueous lithium-ion chemistries *Science* **350** 938–43
[33] Chen L *et al* 2020 A 63 m superconcentrated aqueous electrolyte for high-energy Li-Ion batteries *ACS Energy Lett.* **5** 968–74
[34] Liang G, Mo F, Ji X and Zhi C 2021 Non-metallic charge carriers for aqueous batteries *Nat. Rev. Mater.* **6** 109–23
[35] Sun P, Ma L, Zhou W H, Qiu M J, Wang Z L, Chao D L and Mai W 2021 Simultaneous regulation on solvation shell and electrode interface for dendrite-free Zn Ion batteries achieved by a low-cost glucose additive *Angew. Chem., Int. Ed.* **60** 18247–55
[36] Wang D H, Li Q, Zhao Y W, Hong H, Li H F, Huang Z D, Liang G J, Yang Q and Zhi C Y 2022 Insight on organic molecules in aqueous Zn-Ion batteries with an emphasis on the Zn anode regulation *Adv. Energy Mater.* **12** 2102707
[37] Sui Y and Ji X L 2021 Anticatalytic strategies to suppress water electrolysis in aqueous batteries *Chem. Rev.* **121** 6654–95
[38] Yang Q, Li Q, Liu Z X, Wang D H, Guo Y, Li X L, Tang Y C, Li H F, Dong B B and Zhi C Y 2020 Dendrites in Zn-based batteries *Adv. Mater.* **32** 2001854
[39] Tian Y D, Chen S, He Y L, Chen Q W, Zhang L L and Zhang J T 2022 A highly reversible dendrite-free Zn anode via spontaneous galvanic replacement reaction for advanced zinc-iodine batteries *Nano Res. Energy* **1** 9120025
[40] Kundu D, Adams B D, Duffort V, Vajargah S H and Nazar L F 2016 A high-capacity and long-life aqueous rechargeable zinc battery using a metal oxide intercalation cathode *Nat. Energy* **1** 16119
[41] Yi Z H, Chen G Y, Hou F, Wang L Q and Liang J 2021 Strategies for the stabilization of Zn metal anodes for Zn-Ion batteries *Adv. Energy Mater.* **11** 2003065
[42] Zhang W D, Zhuang H L, Fan L, Gao L N and Lu Y Y 2018 A "cation-anion regulation" synergistic anode host for dendrite-free lithium metal batteries *Sci. Adv.* **4** eaar4410
[43] Li Q, Wang Y B, Mo F N, Wang D H, Liang G J, Zhao Y W, Yang Q, Huang Z D and Zhi C Y 2021 Calendar life of Zn batteries based on Zn anode with Zn powder/current collector structure *Adv. Energy Mater.* **11** 2003931
[44] Wang S-B, Ran Q, Yao R-Q, Shi H, Wen Z, Zhao M, Lang X-Y and Jiang Q 2020 Lamella-nanostructured eutectic zinc–aluminum alloys as reversible and dendrite-free anodes for aqueous rechargeable batteries *Nat. Commun.* **11** 1634
[45] Yang Q, Liang G J, Guo Y, Liu Z X, Yan B X, Wang D H, Huang Z D, Li X L, Fan J and Zhi C Y 2019 Do zinc dendrites exist in neutral zinc batteries: a developed electrohealing strategy to in situ rescue in-service batteries *Adv. Mater.* **31** 1903778
[46] Ma L, Schroeder M A, Borodin O, Pollard T P, Ding M S, Wang C S and Xu K 2020 Realizing high zinc reversibility in rechargeable batteries *Nat. Energy* **5** 743–9
[47] Huang Z D *et al* 2022 Small-dipole-molecule-containing electrolytes for high-voltage aqueous rechargeable batteries *Adv. Mater.* **34** 2106180
[48] Lv Y Q, Xiao Y, Ma L T, Zhi C Y and Chen S M 2022 Recent advances in electrolytes for "beyond aqueous" zinc-ion batteries *Adv. Mater.* **34** 2106409
[49] Yuan L B, Hao J N, Kao C-C, Wu C, Liu H-K, Dou S-X and Qiao S-Z 2021 Regulation methods for the Zn/electrolyte interphase and the effectiveness evaluation in aqueous Zn-ion batteries *Energy Environ. Sci.* **14** 5669–89
[50] Schmeisser M, Illner P, Puchta R, Zahl A and Van Eldik R 2012 Gutmann donor and acceptor numbers for ionic liquids *Chem. Eur. J.* **18** 10969–82
[51] Miranda-Quintana R A and Smiatek J 2021 Calculation of donor numbers: computational estimates for the Lewis basicity of solvents *J. Mol. Liq.* **322** 114506
[52] Fawcett W R 1993 Acidity and basicity scales for polar solvents *J. Phys. Chem.* **97** 9540–6
[53] Liu Z X, Huang Y, Huang Y, Yang Q, Li X L, Huang Z D and Zhi C Y 2020 Voltage issue of aqueous rechargeable metal-ion batteries *Chem. Soc. Rev.* **49** 180–232
[54] Nam K W, Kim H, Choi J H and Choi J W 2019 Crystal water for high performance layered manganese oxide cathodes in aqueous rechargeable zinc batteries *Energy Environ. Sci.* **12** 1999–2009
[55] Cui J, Liu X Y, Xie Y H, Wu K, Wang Y Q, Liu Y Y, Zhang J J, Yi J and Xia Y Y 2020 Improved electrochemical reversibility of Zn plating/stripping: a promising approach to suppress water-induced issues

through the formation of H-bonding *Mater. Today Energy* **18** 100563

[56] Zhang Q, Xia K X, Ma Y L, Lu Y, Li L, Liang J, Chou S L and Chen J 2021 Chaotropic anion and fast-kinetics cathode enabling low-temperature aqueous Zn batteries *ACS Energy Lett.* **6** 2704–12

[57] Sun K E K, Hoang T K A, Doan T N L, Yu Y and Chen P 2018 Highly sustainable zinc anodes for a rechargeable hybrid aqueous battery *Chem. Eur. J.* **24** 1667–73

[58] Cao J, Zhang D D, Zhang X Y, Zeng Z Y, Qin J Q and Huang Y H 2022 Strategies of regulating Zn^{2+} solvation structures for dendrite-free and side reaction-suppressed zinc-ion batteries *Energy Environ. Sci.* **15** 499–528

[59] Cao L S, Li D, Hu E Y, Xu J J, Deng T, Ma L, Wang Y, Yang X-Q and Wang C S 2020 Solvation structure design for aqueous Zn metal batteries *J. Am. Chem. Soc.* **142** 21404–9

[60] Hou Z, Tan H, Gao Y, Li M H, Lu Z H and Zhang B 2020 Tailoring desolvation kinetics enables stable zinc metal anodes *J. Mater. Chem.* A **8** 19367–74

[61] Wang N, Yang Y, Qiu X, Dong X L, Wang Y G and Xia Y Y 2020 Stabilized rechargeable aqueous zinc batteries using ethylene glycol as water blocker *ChemSusChem* **13** 5556–64

[62] Du H H, Wang K, Sun T J, Shi J Q, Zhou X Z, Cai W S and Tao Z L 2022 Improving zinc anode reversibility by hydrogen bond in hybrid aqueous electrolyte *Chem. Eng. J.* **427** 131705

[63] Zhang Q, Ma Y L, Lu Y, Zhou X Z, Lin L, Li L, Yan Z H, Zhao Q, Zhang K and Chen J 2021 Designing anion-type water-free Zn^{2+} solvation structure for robust Zn metal anode *Angew. Chem., Int. Ed.* **60** 23357–64

[64] Wang P J, Xie X S, Xing Z Y, Chen X H, Fang G Z, Lu B G, Zhou J, Liang S Q and Fan H J 2021 Mechanistic insights of Mg^{2+}-electrolyte additive for high-energy and long-life zinc-ion hybrid capacitors *Adv. Energy Mater.* **11** 2101158

[65] Jin Y, Han K S, Shao Y Y, Sushko M L, Xiao J, Pan H L and Liu J 2020 Stabilizing zinc anode reactions by polyethylene oxide polymer in mild aqueous electrolytes *Adv. Funct. Mater.* **30** 2003932

[66] Feng D D, Cao F Q, Hou L, Li T Y, Jiao Y C and Wu P Y 2021 Immunizing aqueous Zn batteries against dendrite formation and side reactions at various temperatures via electrolyte additives *Small* **17** 2103195

[67] Shi J Q, Xia K X, Liu L J, Liu C, Zhang Q, Li L, Zhou X Z, Liang J and Tao Z L 2020 Ultrahigh coulombic efficiency and long-life aqueous Zn anodes enabled by electrolyte additive of acetonitrile *Electrochim. Acta* **358** 136937

[68] Song X Y, He H B, Aboonasr Shiraz M H, Zhu H Z, Khosrozadeh A and Liu J 2021 Enhanced reversibility and electrochemical window of Zn-ion batteries with an acetonitrile/water-in-salt electrolyte *Chem. Commun.* **57** 1246–9

[69] Etman A S, Carboni M, Sun J L and Younesi R 2020 Acetonitrile-based electrolytes for rechargeable zinc batteries *Energy Technol.* **8** 2000358

[70] Hao J N, Yuan L B, Ye C, Chao D L, Davey K, Guo Z P and Qiao S-Z 2021 Boosting zinc electrode reversibility in aqueous electrolytes by using low-cost antisolvents *Angew. Chem., Int. Ed.* **60** 7366–75

[71] Qin R Z *et al* 2021 Tuning Zn^{2+} coordination environment to suppress dendrite formation for high-performance Zn-ion batteries *Nano Energy* **80** 105478

[72] Feng R F, Chi X W, Qiu Q L, Wu J, Huang J Q, Liu J J and Liu Y 2021 Cyclic ether-water hybrid electrolyte-guided dendrite-free lamellar zinc deposition by tuning the solvation structure for high-performance aqueous zinc-ion batteries *ACS Appl. Mater. Interfaces* **13** 40638–47

[73] Nigatu T A, Bezabh H K, Taklu B W, Olbasa B W, Weng Y-T, Wu S-H, Su W-N, Yang C-C and Hwang B J 2021 Synergetic effect of water-in-bisalt electrolyte and hydrogen-bond rich additive improving the performance of aqueous batteries *J. Power Sources* **511** 230413

[74] Dong Y, Miao L C, Ma G Q, Di S L, Wang Y Y, Wang L B, Xu J Z and Zhang N 2021 Non-concentrated aqueous electrolytes with organic solvent additives for stable zinc batteries *Chem. Sci.* **12** 5843–52

[75] Luo M H, Wang C Y, Lu H T, Lu Y H, Xu B B, Sun W P, Pan H G, Yan M and Jiang Y Z 2021 Dendrite-free zinc anode enabled by zinc-chelating chemistry *Energy Storage Mater.* **41** 515–21

[76] Wang N *et al* 2021 Tridentate citrate chelation towards stable fiber zinc-polypyrrole battery with hybrid mechanism *Energy Storage Mater.* **43** 585–94

[77] Hou Z G, Dong M F, Xiong Y L, Zhang X Q, Ao H S, Liu M K, Zhu Y C and Qian Y T 2020 A high-energy and long-life aqueous Zn/birnessite battery via reversible water and Zn^{2+} coinsertion *Small* **16** 2001228

[78] Wang S N, Li T Y, Yin Y B, Chang N N, Zhang H M and Li X F 2022 High-energy-density aqueous zinc-based hybrid supercapacitor-battery with uniform zinc deposition achieved by multifunctional decoupled additive *Nano Energy* **96** 107120

[79] Chen J Z, Zhou W J, Quan Y H, Liu B, Yang M, Chen M F, Han X, Xu X W, Zhang P X and Shi S Q 2022 Ionic liquid additive enabling anti-freezing aqueous electrolyte and dendrite-free Zn metal electrode with organic/inorganic hybrid solid electrolyte interphase layer *Energy Storage Mater.* **53** 629–37

[80] Zhang H W, Zhong Y, Li J B, Liao Y Q, Zeng J L, Shen Y, Yuan L X, Li Z and Huang Y H 2023 Inducing the preferential growth of Zn (002) plane for long cycle aqueous Zn-Ion batteries *Adv. Energy Mater.* **13** 2203254

[81] Huang C, Zhao X, Liu S, Hao Y S, Tang Q L, Hu A P, Liu Z X and Chen X H 2021 Stabilizing zinc anodes by regulating the electrical double layer with saccharin anions *Adv. Mater.* **33** 2100445

[82] Xi M R, Liu Z J, Ding J, Cheng W H, Jia D Z and Lin H 2021 Saccharin anion acts as a "traffic Assistant" of Zn^{2+} to achieve a long-life and dendritic-free zinc plate anode *ACS Appl. Mater. Interfaces* **13** 29631–40

[83] Zeng X *et al* 2021 Bio-inspired design of an in situ multifunctional polymeric solid-electrolyte interphase for Zn metal anode cycling at 30 mA cm^{-2} and 30 mA h cm^{-2} *Energy Environ. Sci.* **14** 5947–57

[84] Ding F *et al* 2013 Dendrite-free lithium deposition via self-healing electrostatic shield mechanism *J. Am. Chem. Soc.* **135** 4450–6

[85] Wan F, Zhang L L, Dai X, Wang X Y, Niu Z Q and Chen J 2018 Aqueous rechargeable zinc/sodium vanadate batteries with enhanced performance from simultaneous insertion of dual carriers *Nat. Commun.* **9** 1656

[86] Hoang T K A, Acton M, Chen H T H, Huang Y, Doan T N L and Chen P 2017 Sustainable gel electrolyte containing Pb^{2+} as corrosion inhibitor and dendrite suppressor for the zinc anode in the rechargeable hybrid aqueous battery *Mater. Today Energy* **4** 34–40

[87] Li Y, Wu P, Zhong W, Xie C, Xie Y, Zhang Q, Sun D, Tang Y and Wang H 2021 A progressive nucleation mechanism enables stable zinc stripping-plating behavior *Energy Environ. Sci.* **14** 5563–71

[88] Yan M D, Xu C L, Sun Y, Pan H L and Li H 2021 Manipulating Zn anode reactions through salt anion involving hydrogen bonding network in aqueous electrolytes with PEO additive *Nano Energy* **82** 105739

[89] Zhou T Y *et al* 2022 Toward stable zinc aqueous rechargeable batteries by anode morphology modulation via polyaspartic acid additive *Energy Storage Mater.* **45** 777–85

[90] Wu Y *et al* 2023 Polymer chain-guided Ion transport in aqueous electrolytes of Zn-Ion batteries *Adv. Energy Mater.* **13** 2300719

[91] Zhang Q, Luan J Y, Fu L, Wu S G, Tang Y G, Ji X B and Wang H Y 2019 The three-dimensional dendrite-free zinc anode on a copper mesh with a zinc-oriented polyacrylamide electrolyte additive *Angew. Chem.* **131** 15988–94

[92] Peng M K, Tang X N, Xiao K, Hu T, Yuan K and Chen Y W 2023 Polycation-regulated electrolyte and interfacial electric fields for stable zinc metal batteries *Angew. Chem., Int. Ed.* **62** e202302701

[93] Chen Z H, Chen H Z, Che Y C, Cheng L, Zhang H, Chen J, Xie F Y, Wang N, Jin Y S and Meng H 2021 Arginine cations inhibiting charge accumulation of dendrites and boosting Zn metal reversibility in aqueous rechargeable batteries *ACS Sustain. Chem. Eng.* **9** 6855–63

[94] Bayaguud A, Luo X, Fu Y P and Zhu C B 2020 Cationic surfactant-type electrolyte additive enables three-dimensional dendrite-free zinc anode for stable zinc-ion batteries *ACS Energy Lett.* **5** 3012–20

[95] Zhang S-J, Hao J N, Luo D, Zhang P-F, Zhang B K, Davey K, Lin Z and Qiao S-Z 2021 Dual-function electrolyte additive for highly reversible Zn anode *Adv. Energy Mater.* **11** 2102010

[96] Xu W N, Zhao K N, Huo W C, Wang Y Z, Yao G, Gu X, Cheng H W, Mai L, Hu C G and Wang X D 2019 Diethyl ether as self-healing electrolyte additive enabled long-life rechargeable aqueous zinc ion batteries *Nano Energy* **62** 275–81

[97] Wei T T, Ren Y K, Wang Y F, Mo L, Li Z Q, Zhang H, Hu L H and Cao G Z 2023 Addition of Dioxane in electrolyte promotes (002)-textured zinc growth and suppressed side reactions in Zinc-Ion batteries *ACS Nano* **17** 3765–75

[98] Zhang N, Cheng F Y, Liu J X, Wang L B, Long X H, Liu X S, Li F J and Chen J 2017 Rechargeable aqueous zinc-manganese dioxide batteries with high energy and power densities *Nat. Commun.* **8** 405

[99] Zhu C Y, Fang G Z, Liang S Q, Chen Z X, Wang Z Q, Ma J Y, Wang H, Tang B Y, Zheng X S and Zhou J 2020 Electrochemically induced cationic defect in MnO intercalation cathode for aqueous zinc-ion battery *Energy Storage Mater.* **24** 394–401

[100] Fang G Z, Zhu C Y, Chen M H, Zhou J, Tang B Y, Cao X X, Zheng X S, Pan A Q and Liang S Q 2019 Suppressing manganese dissolution in potassium manganate with rich oxygen defects engaged high-energy-density and durable aqueous Zinc-Ion battery *Adv. Funct. Mater.* **29** 1808375

[101] Guo S, Liang S Q, Zhang B S, Fang G Z, Ma D and Zhou J 2019 Cathode interfacial layer formation *via in situ* electrochemically charging in aqueous zinc-ion battery *ACS Nano* **13** 13456–64

[102] Liu F, Chen Z X, Fang G Z, Wang Z Q, Cai Y S, Tang B Y, Zhou J and Liang S Q 2019 V_2O_5 nanospheres with mixed vanadium valences as high electrochemically active aqueous Zinc-Ion battery cathode *Nano-Micro. Lett.* **11** 25

[103] Chuai M Y *et al* 2022 Theory-driven design of a cationic accelerator for high-performance electrolytic MnO_2–Zn batteries *Adv. Mater.* **34** 2203249

[104] Guo X, Zhou J, Bai C L, Li X K, Fang G Z and Liang S Q 2020 Zn/MnO_2 battery chemistry with dissolution-deposition mechanism *Mater. Today Energy* **16** 100396

[105] Soundharrajan V *et al* 2018 Aqueous magnesium zinc hybrid battery: an advanced high-voltage and high-energy $MgMn_2O_4$ cathode *ACS Energy Lett.* **3** 1998–2004

[106] Wang D H, Wang L F, Liang G J, Li H F, Liu Z X, Tang Z J, Liang J B and Zhi C Y 2019 A superior δ-MnO_2 cathode and a self-healing Zn-δ-MnO_2 battery *ACS Nano* **13** 10643–52

[107] Zheng X H *et al* 2021 Boosting electrolytic MnO_2-Zn batteries by a bromine mediator *Nano Lett.* **21** 8863–71

[108] Zhu K Y, Wu T and Huang K 2021 Understanding the dissolution and phase transformation mechanisms in aqueous Zn/α-V_2O_5 batteries *Chem. Mater.* **33** 4089–98

[109] Lu Y Y, Zhu T Y, Van Den Bergh W, Stefik M and Huang K 2020 A high performing Zn-Ion battery cathode enabled by in situ transformation of V_2O_5 atomic layers *Angew. Chem., Int. Ed.* **59** 17004–11

[110] Yang G Z, Li Q, Ma K X, Hong C and Wang C X 2020 The degradation mechanism of vanadium oxide-based aqueous zinc-ion batteries *J. Mater. Chem.* A **8** 8084–95

[111] Guo N *et al* 2022 A review on 3D zinc anodes for zinc ion batteries *Small Methods* **6** 2200597

[112] Yan H H, Zhang X K, Yang Z W, Xia M T, Xu C W, Liu Y W, Yu H X, Zhang L Y and Shu J 2022 Insight into the electrolyte strategies for aqueous zinc ion batteries *Coord. Chem. Rev.* **452** 214297

[113] Roy B, Pal U, Kar M and MacFarlane D R 2022 Recent strategies for improving the performance of ionic liquids as battery electrolytes *Curr. Opin. Green Sustain. Chem.* **37** 100676

[114] Zong Y, He H W, Wang Y Z, Wu M H, Ren X C, Bai Z C, Wang N N, Ning X and Dou S X 2023 Functionalized separator strategies toward advanced aqueous zinc-ion batteries *Adv. Energy Mater.* **13** 2300403

[115] Li X L, Huang Z D, Shuck C E, Liang G J, Gogotsi Y and Zhi C Y 2022 MXene chemistry, electrochemistry and energy storage applications *Nat. Rev. Chem.* **6** 389–404

[116] Li H F, Ma L T, Han C P, Wang Z F, Liu Z X, Tang Z J and Zhi C Y 2019 Advanced rechargeable zinc-based batteries: recent progress and future perspectives *Nano Energy* **62** 550–87

[117] Fan X L and Wang C S 2021 High-voltage liquid electrolytes for Li batteries: progress and perspectives *Chem. Soc. Rev.* **50** 10486–566

[118] Geng Y F *et al* 2022 Electrolyte additive engineering for aqueous Zn ion batteries *Energy Storage Mater.* **51** 733–55

[119] Zhang T S, Tang Y, Guo S, Cao X X, Pan A Q, Fang G Z, Zhou J and Liang S Q 2020 Fundamentals and perspectives in developing zinc-ion battery electrolytes: a comprehensive review *Energy Environ. Sci.* **13** 4625–65

[120] Cao X *et al* 2019 Monolithic solid–electrolyte interphases formed in fluorinated orthoformate-based electrolytes minimize Li depletion and pulverization *Nat. Energy* **4** 796–805

[121] Tang B Y, Shan L T, Liang S Q and Zhou J 2019 Issues and opportunities facing aqueous zinc-ion batteries *Energy Environ. Sci.* **12** 3288–304

[122] Ming J, Guo J, Xia C, Wang W X and Alshareef H N 2019 Zinc-ion batteries: materials, mechanisms, and applications *Mater. Sci. Eng.* R **135** 58–84

[123] Li C P, Xie X S, Liang S Q and Zhou J 2020 Issues and future perspective on zinc metal anode for rechargeable aqueous zinc-ion batteries *Energy Environ. Mater.* **3** 146–59